K decreases in HCC, the PIVKA-II production increases (20). We suspected that the transcription of OATP8 might change in accordance with the decrease of ligands to these receptors. As a result, we expected that PIVKA-II expression and OATP8 expression might be correlated.

However, there were many patients that showed low AFP and PIVKA-II expression in hypointense HCCs. We attribute this to the fact that OATP8, AFP, and PIVKA-II have several direct and indirect regulatory mechanisms other than the hepatocyte nuclear factor route (21). Further investigation is needed to clarify the real underlying molecular biology of these correlations.

The molecular classification of subtypes of HCCs is now being investigated by several groups (22). Yamashita et al (23,24) reported on HCC subtypes that were classified on the basis of expression of AFP and epithelial cell adhesion molecule, a stem cell marker. According to their reports, AFP-positive and epithelial cell adhesion molecule–positive HCCs showed stem and progenitor cell features with invasive character and poor prognosis compared with AFP-negative and epithelial cell adhesion molecule–negative HCCs that demonstrated mature hepatocyte-like features with a relatively good prognosis. These features of AFP-negative and epithelial cell adhesion molecule–negative HCCs resembled those of hyperintense HCCs, and we surmised that the origin of hyperintense HCC may be mature hepatocyte-like cells rather than stem or progenitor cells. We think that hyperintense HCCs may have some specific molecular or genetic profiles. Further molecular and genetic analyses are needed to clarify the exact molecular biologic basis for this possible subtype of HCCs.

Our study had limitations. First, the total number of hyperintense HCCs examined was small because such tumors are relatively rare (8). Second, we only assessed HCC lesions that were hypervascular in the arterial phase, and therefore our results cannot be applied to a general screening population with benign disease, hypovascular HCC on arterial-phase images, or other malignancies. Third, there was a variability of the imaging parameters, such as strength of magnetic field, section thickness, and on imaging timing, because this was multicenter study.

In conclusion, hyperintense HCCs on hepatobiliary phase images showed significantly higher differentiation grades, less frequent portal vein invasion, and lower recurrence rates than did hypointense HCCs. Moreover, hyperintense HCCs showed significantly lower expression of AFP and PIVKA-II than did hypointense HCCs. Hyperintense HCCs on hepatobiliary phase gadoxetic acid–enhanced MR images may be a particular form of hypervascular HCC with biologically less aggressive features than those of hypointense HCCs.

Acknowledgments: We deeply appreciate Dr. Taro Yamashita (Department of Gastroenterology, Kanazawa University Graduate School of Medical Science, Kanazawa, Japan), Dr. Yoh Zen (Institute of Liver Studies, King's College Hospital, London, United Kingdom) and Dr. Seiko Kitamura-Sawada (Division of Pathology, Kanazawa University Hospital, Kanazawa, Japan) for their support to our study.

Disclosures of Conflicts of Interest: A.K. No relevant conflicts of interest to disclose. **O.M.** Financial activities related to the present article: Received a consulting fee or honorarium and fees for participation in review activities from Bayer Japan. Financial activities not related to the present article: none to disclose. Other relationships: none to disclose. **N.Y.** No relevant conflicts of interest to disclose. **K.K.** No relevant conflicts of interest to disclose. **S.Kobayashi.** No relevant conflicts of interest to disclose. **W.K.** No relevant conflicts of interest to disclose. **T.G.** No relevant conflicts of interest to disclose. **T.Y.** No relevant conflicts of interest to disclose. **S.Kaneko.** No relevant conflicts of interest to disclose. **Y.N.** No relevant conflicts of interest to disclose. **R.K.** No relevant conflicts of interest to disclose. **S.A.** No relevant conflicts of interest to disclose.

References

1. Caldwell S, Park SH. The epidemiology of hepatocellular cancer: from the perspectives of public health problem to tumor biology. J Gastroenterol 2009;44(Suppl 19):96–101.
2. Ahn SS, Kim MJ, Lim JS, Hong HS, Chung YE, Choi JY. Added value of gadoxetic acid-enhanced hepatobiliary phase MR imaging in the diagnosis of hepatocellular carcinoma. Radiology 2010;255(2):459–466.
3. Ichikawa T, Saito K, Yoshioka N, et al. Detection and characterization of focal liver lesions: a Japanese phase III, multicenter comparison between gadoxetic acid disodium-enhanced magnetic resonance imaging and contrast-enhanced computed tomography predominantly in patients with hepatocellular carcinoma and chronic liver disease. Invest Radiol 2010;45(3):133–141.
4. Golfieri R, Renzulli M, Lucidi V, Corcioni B, Trevisani F, Bolondi L. Contribution of the hepatobiliary phase of Gd-EOB-DTPA-enhanced MRI to Dynamic MRI in the detection of hypovascular small (≤ 2 cm) HCC in cirrhosis. Eur Radiol 2011;21(6):1233–1242.
5. Kitao A, Zen Y, Matsui O, et al. Hepatocellular carcinoma: signal intensity at gadoxetic acid-enhanced MR Imaging—correlation with molecular transporters and histopathologic features. Radiology 2010;256(3):817–826.
6. Narita M, Hatano E, Arizono S, et al. Expression of OATP1B3 determines uptake of Gd-EOB-DTPA in hepatocellular carcinoma. J Gastroenterol 2009;44(7):793–798.
7. Asayama Y, Tajima T, Nishie A, et al. Uptake of Gd-EOB-DTPA by hepatocellular carcinoma: radiologic-pathologic correlation with special reference to bile production. Eur J Radiol 2011;80(3):e243–e248.
8. Kitao A, Matsui O, Yoneda N, et al. The uptake transporter OATP8 expression decreases during multistep hepatocarcinogenesis: correlation with gadoxetic acid enhanced MR imaging. Eur Radiol 2011;21(10):2056–2066.
9. Jung D, Hagenbuch B, Gresh L, Pontoglio M, Meier PJ, Kullak-Ublick GA. Characterization of the human OATP-C (SLC21A6) gene promoter and regulation of liver-specific OATP genes by hepatocyte nuclear factor 1 alpha. J Biol Chem 2001;276(40):37206–37214.
10. Inagaki Y, Tang W, Xu H, et al. Des-gamma-carboxyprothrombin: clinical effectiveness and biochemical importance. Biosci Trends 2008;2(2):53–60.
11. Miyaaki H, Nakashima O, Kurogi M, Eguchi K, Kojiro M. Lens culinaris agglutinin-reactive alpha-fetoprotein and protein induced by vitamin K absence II are potential indicators of a poor prognosis: a histopathological study of surgically resected hepatocellular carcinoma. J Gastroenterol 2007;42(12):962–968.
12. Nakabayashi H, Koyama Y, Suzuki H, et al. Functional mapping of tissue-specific elements of the human alpha-fetoprotein gene enhancer. Biochem Biophys Res Commun 2004;318(3):773–785.

13. Ishii K, Yoshida Y, Akechi Y, et al. Hepatic differentiation of human bone marrow-derived mesenchymal stem cells by tetracycline-regulated hepatocyte nuclear factor 3beta. Hepatology 2008;48(2):597–606.

14. Hirohashi S, Ishak KG, Kojiro M, et al. Hepatocellular carcinoma. In: Hamilton SR, Aaltonen LA, eds. Pathology and genetics of tumours of the digestive system. Lyon, France: IARC, 2000; 157–172.

15. International Consensus Group for Hepatocellular Neoplasia. Pathologic diagnosis of early hepatocellular carcinoma: a report of the international consensus group for hepatocellular neoplasia. Hepatology 2009;49(2):658–664.

16. Liver Cancer Study Group of Japan. General rules for the clinical and pathological study of primary liver cancer. 3rd ed. Tokyo, Japan: Kanehara, 2010.

17. Vavricka SR, Jung D, Fried M, Grützner U, Meier PJ, Kullak-Ublick GA. The human organic anion transporting polypeptide 8 (SLCO1B3) gene is transcriptionally repressed by hepatocyte nuclear factor 3beta in hepatocellular carcinoma. J Hepatol 2004;40(2):212–218.

18. Gui C, Miao Y, Thompson L, et al. Effect of pregnane X receptor ligands on transport mediated by human OATP1B1 and OATP1B3. Eur J Pharmacol 2008;584(1):57–65.

19. Azuma K, Urano T, Ouchi Y, Inoue S. Vitamin K2 suppresses proliferation and motility of hepatocellular carcinoma cells by activating steroid and xenobiotic receptor. Endocr J 2009;56(7):843–849.

20. Huisse MG, Leclercq M, Belghiti J, et al. Mechanism of the abnormal vitamin K-dependent gamma-carboxylation process in human hepatocellular carcinomas. Cancer 1994;74(5):1533–1541.

21. Saito S, Ojima H, Ichikawa H, Hirohashi S, Kondo T. Molecular background of alpha-fetoprotein in liver cancer cells as revealed by global RNA expression analysis. Cancer Sci 2008;99(12):2402–2409.

22. Lee JS, Heo J, Libbrecht L, et al. A novel prognostic subtype of human hepatocellular carcinoma derived from hepatic progenitor cells. Nat Med 2006;12(4):410–416.

23. Yamashita T, Ji J, Budhu A, et al. EpCAM-positive hepatocellular carcinoma cells are tumor-initiating cells with stem/progenitor cell features. Gastroenterology 2009;136(3):1012–1024.

24. Yamashita T, Forgues M, Wang W, et al. EpCAM and alpha-fetoprotein expression defines novel prognostic subtypes of hepatocellular carcinoma. Cancer Res 2008;68(5):1451–1461.

HEPATOLOGY
Official Journal of the American Association for the Study of Liver Diseases

Transcriptomic Profiling Reveals Hepatic Stem-Like Gene Signatures and Interplay of miR-200c and Epithelial-Mesenchymal Transition in Intrahepatic Cholangiocarcinoma

Naoki Oishi,[1] Mia R. Kumar,[1] Stephanie Roessler,[1] Junfang Ji,[1] Marshonna Forgues,[1] Anuradha Budhu,[1] Xuelian Zhao,[1] Jesper B. Andersen,[2] Qing-Hai Ye,[3] Hu-Liang Jia,[3] Lun-Xiu Qin,[3] Taro Yamashita,[4] Hyun Goo Woo,[5] Yoon Jun Kim,[6] Shuichi Kaneko,[4] Zhao-You Tang,[3] Snorri S. Thorgeirsson,[2] and Xin Wei Wang[1]

Intrahepatic cholangiocellular carcinoma (ICC) is the second most common type of primary liver cancer. However, its tumor heterogeneity and molecular characteristics are largely unknown. In this study, we conducted transcriptomic profiling of 23 ICC and combined hepatocellular cholangiocarcinoma tumor specimens from Asian patients using Affymetrix messenger RNA (mRNA) and NanoString microRNA microarrays to search for unique gene signatures linked to tumor subtypes and patient prognosis. We validated the signatures in an additional 68 ICC cases derived from Caucasian patients. We found that both mRNA and microRNA expression profiles could independently classify Asian ICC cases into two main subgroups, one of which shared gene expression signatures with previously identified hepatocellular carcinoma (HCC) with stem cell gene expression traits. ICC-specific gene signatures could predict survival in Asian HCC cases and independently in Caucasian ICC cases. Integrative analyses of the ICC-specific mRNA and microRNA expression profiles revealed that a common signaling pathway linking miR-200c signaling to epithelial-mesenchymal transition (EMT) was preferentially activated in ICC with stem cell gene expression traits. Inactivation of miR-200c resulted in an induction of EMT, whereas activation of miR-200c led to a reduction of EMT including a reduced cell migration and invasion in ICC cells. We also found that miR-200c and neural cell adhesion molecule 1 (NCAM1) expression were negatively correlated and their expression levels were predictive of survival in ICC samples. NCAM1, a known hepatic stem/progenitor cell marker, was experimentally demonstrated to be a direct target of miR-200c. Conclusion: Our results indicate that ICC and HCC share common stem-like molecular characteristics and poor prognosis. We suggest that the specific components of EMT may be exploited as critical biomarkers and clinically relevant therapeutic targets for an aggressive form of stem cell-like ICC. (HEPATOLOGY 2012;56:1792-1803)

Primary liver cancer (PLC) is the second most lethal cancer for men in the world.[1] Intrahepatic cholangiocellular carcinoma (ICC) is the second most common type of PLC. Although ICC is much less common than hepatocellular carcinoma (HCC), its incidence has increased drastically over the past two decades.[2,3] However, the molecular pathogenesis of ICC is largely unknown. Understanding of the tumor

Abbreviations: CHC, combined hepatocellular cholangiocarcinoma; CSC, cancer stem cell; EMT, epithelial-mesenchymal transition; FNH, focal nodular hyperplasia; GEO, gene expression omnibus; HCC, hepatocellular carcinoma; HpSC-ICC, hepatic stem cell-like ICC; ICC, intrahepatic cholangiocarcinoma; MH-ICC, mature hepatocyte-like ICC; PLC, primary liver cancer; x-HCC; extreme HCC.

From the [1]Laboratory of Human Carcinogenesis, Center for Cancer Research, National Cancer Institute, National Institutes of Health, Bethesda, MD; [2]Laboratory of Experimental Carcinogenesis, Center for Cancer Research, National Cancer Institute, National Institutes of Health, Bethesda, MD; [3]Liver Cancer Institute, Fudan University, Shanghai, China; [4]Liver Disease Center and Kanazawa University Hospital, Kanazawa University, Kanazawa, Japan; [5]Department of Physiology, Ajou University School of Medicine, Suwon, Korea; and [6]Department of Internal Medicine and Liver Research Institute, Seoul National University College of Medicine, Seoul, Korea.

Received December 22, 2011; accepted May 19, 2012.

Supported in part by the Intramural Research Program of the center for Cancer Research, the U.S. National Cancer Institute (Z01 BC 010313 and Z01 BC 010876).

Dr. Mia R. Kumar is currently affiliated with Human Genome Sciences, Rockville, MD.

biology of HCC and ICC that contributes to tumor heterogeneity is paramount in developing effective therapies to improve patient outcome.

The cellular origin of HCC and ICC has been subject to intense debate in recent years. It is thought that HCC is derived from hepatocytes, whereas ICC arises from intrahepatic biliary epithelium. However, a mixed form of HCC and ICC, also known as combined hepatocellular cholangiocarcinoma (CHC), has been described to have distinct clinicopathological features but morphological intermediates of HCC and ICC, suggesting that HCC and ICC could share the same cellular origin.[4-6] Recent studies utilizing high-resolution genomic approaches have shed light on the revelation of cellular origin of HCC and suggest that a subset of HCC contains stem cell-like features.[7-10] For example, a subset of tumor cells isolated from HCC patients are tumor-initiating cells with stem cell traits.[11-14] Moreover, HCC may share an ICC-like gene expression trait.[15] These results are consistent with the cancer stem cell (CSC) hypothesis, which suggests that most tumor cells are derived from undifferentiated cells with stem-like capabilities and that both ICC and HCC may share the same cellular origin of hepatic stem/progenitor cells.

Global messenger RNA (mRNA) and microRNA profiling approaches have been proven to be effective in identifying genes critical to HCC.[8,9,16-22] In this study, we used both mRNA and microRNA profiling approaches to determine tumor heterogeneity and molecular characteristics of ICC. We found that ICC samples consist of at least two main subtypes that share similar molecular activities, with HCC linked to stem cell-like gene expression and patient survival. Integrative genomic analyses revealed that genes and microRNAs involved in epithelial-mesenchymal transition (EMT) are altered in stem-like ICCs. Our results shed light on ICC diagnosis and may open new avenues for therapeutic interventions for targeting poor prognosis ICC patients.

Materials and Methods

Human Subjects. ICC and CHC tissues were obtained with informed consent from Asian patients who underwent curative resection between 2002 and 2003 at the Liver Cancer Institute and Zhongshan Hospital (Fudan University, Shanghai, China) and between 2008 and 2010 at the Kanazawa University Hospital (Ishikawa, Japan). Sample collection was approved by the Institutional Review Board of the corresponding institutes and recorded by the National Institutes of Health (NIH) Office of Human Subjects Research. A total of 23 ICC and CHC cases were used to build mRNA and microRNA signatures. The initial diagnosis was made based on serological test and imaging, and was confirmed histopathologically by pathologists. The characteristics of 68 Caucasian ICC patients from an independent cohort were described recently.[23]

Cell Line, Culture, and Transfection. HuCCT1 and HUH28 cell lines were used for miR-200c functional studies. These cell lines were obtained from the Japanese Collection of Research Bioresources Cell Bank and were cultured in RPMI supplemented with 10% fetal bovine serum, 100 U/mL penicillin, 0.1 mg/mL streptomycin, and 2 mmol/L L-glutamine. An immortalized human cholangiocyte-derived cell line, H69, kindly provided by Dr. Gregory Gores (Mayo Clinic), was cultured as described.[24] A luciferase reporter containing an upstream 0.9-kb fragment of pri-miR-200c was kindly provided by Dr. Li Wang (University of Utah School of Medicine).[25] A detailed description of other transfection reagents, methodologies such as cell culture, cell proliferation and apoptosis assays, luciferase assay, immunohistochemical analysis, and cell migration and invasion assays can be found in the Supporting Materials.

Microarray Processing. Total RNA was extracted from frozen tissue using Trizol (Invitrogen) according to the manufacturer's protocol. Only RNA samples with good RNA quality as confirmed with the Agilent 2100 Bioanalyzer (Agilent Technologies) were included for array study. Gene expression profiling of 23 tumor samples (16 ICC, 7 CHC), as well as seven paired noncancerous liver tissues from ICC patients and seven benign liver lesions (five focal nodular hyperplasia [FNH], two adenoma) was carried out on Affymetrix GeneChip Human Gene-ST 1.0 arrays according to the manufacturer's protocol and processed as described.[26] Affymetrix gene expression arrays obtained from different platforms were combined with the match probes package in R. Raw gene expression data were normalized using the robust multi-array average

Address reprint requests to: Dr. Xin Wei Wang, National Cancer Institute, 37 Convent Dr., Bldg. 37, Rm. 3044A, Bethesda, MD 20892. E-mail: xw3u@nih.gov
Copyright © 2012 by the American Association for the Study of Liver Diseases.
View this article online at wileyonlinelibrary.com.
DOI 10.1002/hep.25890
Potential conflict of interest: Nothing to report.
Additional Supporting Information may be found in the online version of this article.

(RMA) method and global median centering. For genes with more than one probe set, the mean gene expression was calculated. Total RNA was used for the nCounter microRNA platform. All sample preparation and hybridization was performed according to the manufacturer's instructions. All hybridization reactions were incubated at 65°C for a minimum of 12 hours. Hybridized probes were purified and counted on the nCounter Prep Station and Digital Analyzer (NanoString) following the manufacturer's instructions. For each assay a high-density scan was performed. For platform validation using synthetic oligonucleotides, NanoString nCounter microRNA raw data were normalized for lane-to-lane variation with a dilution series of six spike-in positive controls. The sum of the six positive controls for a given lane was divided by the average sum across lanes to yield a normalization factor, which was then multiplied by the raw counts in each lane to give normalized values. Raw mRNA and microRNA data are accessible through the accession numbers GSE32879 and GSE32957 at the NCBI Gene Expression Omnibus (GEO) database. Other statistical methods can be found in the Supporting Materials.

Real-Time Reverse-Transcription Polymerase Chain Reaction (RT-PCR) Analysis. Total RNA was subjected to qRT-PCR. Mature microRNAs and other mRNAs were analyzed using the TaqMan microRNA Assays and Gene Expression Assays, respectively, in accordance with manufacturer's instructions (Applied Biosystems, Foster City, CA). All RT reactions were run in a GeneAmp PCR 9700 Thermocycler (Applied Biosystems). Probes used for the analyses were as follows: ZEB1, Hs00232783_m1; ZEB2, Hs00207691_m1; VIM, Hs00185584_m1; CDH1, Hs01023894_m1; CDH2, Hs00983056_m1; MYC, Hs00905030_m1; Hsa-miR-200c, 002300; Hsa-miR-141, 000463 (Applied Biosystems). The experiments were performed in triplicate. The TaqMan gene assay for 18s and actin was used to normalize the relative abundance of mRNA. RNU6B RNA was used as a control for miR-200c.

Results

Profiling of mRNA Expression in ICC and CHC. We performed transcriptomic analyses of 30 retrospectively collected ICC and CHC clinical specimens from Chinese (n = 13) and Japanese (n = 10) patients with seven paired nontumor liver tissues from ICC patients using Affymetrix GeneChip Human Gene-ST arrays. Five FNH cases and two adenomas were also included as benign tumors of the liver. Clinical features of these ICC and CHC cases are included in Supporting Table S1. Multidimensional scaling analysis revealed that malignant tumor samples were mainly different from benign tumors and nontumor tissues, suggesting that malignant tumors have a vastly different gene expression profile (Fig. S1). To determine tumor heterogeneity, unsupervised hierarchical clustering analysis of 23 ICC and CHC samples based on all genes was conducted. The result revealed that tumor samples can be divided into two main groups, i.e., cluster-A and cluster-B (Fig. 1A). Kaplan-Meier survival analysis revealed that ICC cases in cluster-A had a shorter survival than those in cluster-B (Fig. 1B). These results suggest that gene expression and tumor biology differ significantly among different ICC tumor samples.

We previously identified two HCC subgroups, one resembling gene expression signatures of hepatic stem cells (referred to as HpSC-HCC) and the other similar to mature hepatocyte (referred to as MH-HCC). To determine if ICC subgroups have different gene expression profiles compared to HCC subgroups, we randomly selected two groups of HCC samples, each consisting of 23 age- and gender-matched HCC cases from an existing cohort of 246 HCC samples with available Affymetrix data (GEO accession number GSE14520) and compared them with 23 ICC and CHC tumors (Table S1). Unsupervised hierarchical clustering analysis revealed two main branches. All eight cluster-A ICC samples were grouped with epithelial cell adhesion molecule $(EpCAM)^{+}AFP^{+}$ HCC cases previously identified having a stem cell-like gene expression trait, whereas all eight cluster-B ICC samples were grouped with $EpCAM^{-}AFP^{-}$ HCC cases with a mature hepatocyte-like gene expression trait (Fig. S2A).[9] Similar results were obtained when ICC/CHC cases were compared to a second group of 23 randomly selected HCC cases (Fig. S2B). Seven CHC cases were split among two clusters. For the convenience of keeping track of these ICC samples, we refer to ICC cases in cluster-A as HpSC-ICC (i.e., hepatic stem cell-like ICC) and those in cluster-B as MH-ICC (i.e., mature hepatocyte-like ICC). These results indicate that both ICC and HCC are heterogeneous and their subgroups share similar gene expression profiles.

Next, we performed a class comparison analysis and identified 636 genes that are differentially expressed between eight HpSC-ICC and eight MH-ICC cases (univariate $P < 0.01$; false discovery rate [FDR] <0.2) (Table S2). We then tested whether this 636 ICC-specific gene signature could independently classify HCC

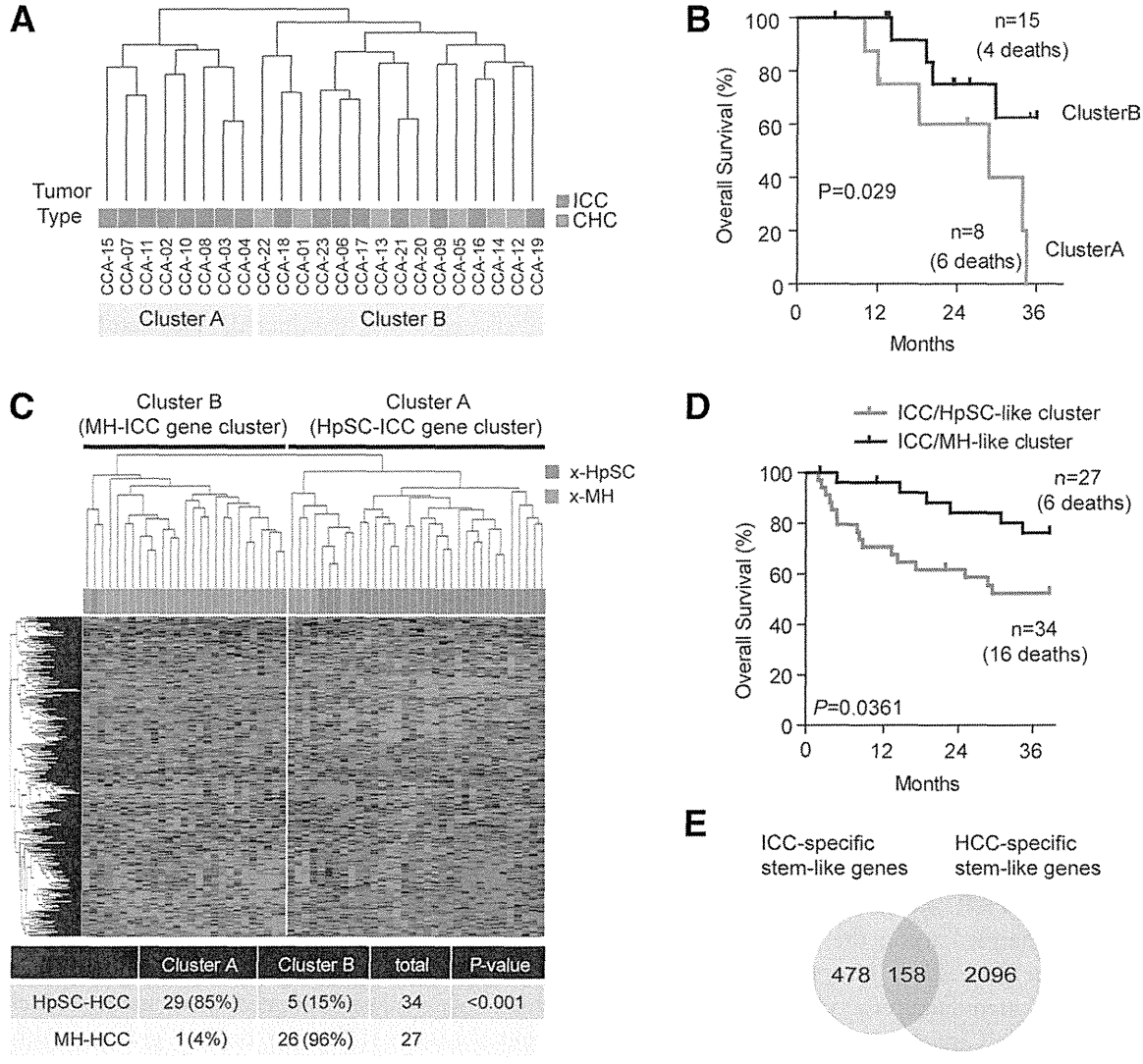

Fig. 1. Heterogeneity of Asian ICC and HCC cases based on mRNA expression profiling. (A) Unsupervised hierarchical clustering of 23 ICC and CHC cases based on global mRNA expression using centered correlation and average linkage. The red and green bars beneath the dendrogram indicate ICC and ICC with CHC features, respectively. ICC cases in cluster-A are referred to as HpSC-ICC and ICC cases in Cluster-B are referred to as MH-ICC. (B) Kaplan-Meier analysis of ICC cases based on the classification of cluster-A and cluster-B from (A). (C) Hierarchical clustering of 61 extreme HCC cases (i.e., 34 *x*-HpSC HCC and 27 *x*-MH HCC) based on the expression of 636 ICC-specific genes. The red and green bars above the heatmap indicate *x*-HpSC and *x*-MH, respectively. A summary of HCC cases based on the dendrogram classification with the ICC-specific signature is included. A chi-squared test was used to determine the correct classification. (D) Kaplan-Meier plot of 61 extreme HCC cases based on the classification by the 636-gene signature into HpSC-ICC and MH-ICC clusters. (E) Venn-diagram of stem-like ICC genes and stem-like HCC genes.

cases based on HpSC-like or MH-like features. We tested the robustness of the signature to discriminate HpSC-HCC from MH-HCC cases by examining 61 well-defined extreme HCC cases or *x*-HCC, i.e., those with top quartile EpCAM expression in HCC tissues and with >1,000 ng/mL of serum alpha-fetoprotein (AFP) levels versus those with bottom quartile EpCAM expression and with <20 ng/mL of serum AFP levels (Table S1). Hierarchical clustering analysis revealed that the 636 ICC-specific genes could nicely divide *x*-HpSC and *x*-MH HCC cases (Fig. 1C) and were associated with HCC survival (Fig. 1D). This 636 ICC-specific gene signature was also associated with survival in 139 remaining unstratified HCC cases from the original 246 HCC cases after excluding 46 randomly selected HCC cases and 61 extreme HCC cases used in the initial clustering analysis (Fig. S2C). Venn diagram analysis indicated that 158 of 636 ICC-specific genes (25%) overlapped with previously identified stem-like HCC genes (Fig. 1E). Consistent with the data in Fig. 1C, 158 overlapping genes could significantly discriminate stem-like HCC cases from mature hepatocyte-like HCC cases ($P < 0.0001$) and was associated with HCC survival ($P = 0.031$)

(Fig. S3). The above data indicate that ICC cases could be classified into two main subtypes that are associated with stem-like or mature hepatocyte like gene expression traits, respectively, and that ICC and HCC may share common gene expression profiles reflecting their cellular origins.

Profiling of MicroRNA Expression in ICC and CHC. We used the NanoString nCounter microRNA Expression Assay platform to independently examine gene expression profiles of the same 23 ICC and CHC samples used above. Unsupervised clustering analysis based on the expression of all 700 human mature microRNAs revealed that ICCs were again divided into two main clusters, where 5 of 6 ICC cases in cluster A belong to HpSC-ICC and 7 of 10 cases in cluster-B belong to MH-ICC as assigned by mRNA expression (Fig. 2A). Class comparison analysis revealed 23 microRNAs to be differentially expressed between HpSC-ICC and MH-ICC ($P < 0.05$) (Table S3). This ICC-specific microRNA signature was further tested for its ability to classify the same HCC cohort described above with available microRNA expression data generated from an independent array platform (GEO accession number: GSE6857). Again, the ICC-specific microRNA signature could significantly discriminate well-defined extreme HCC subgroups and was associated with HCC survival (Fig. 2B,C).

Our results indicate that HpSC-ICC and MH-ICC cases can be independently classified by mRNA and microRNA expression, which suggests that these two subgroups have a clearly measurable difference at the gene expression level. We hypothesized that those HpSC-ICC tumors share the same stem-like traits with HCC with poor survival, and patients with this type of ICC would have a poor outcome. To determine if ICC-specific gene signature is predictive of ICC patient survival, we performed hierarchical clustering analysis using 158 overlapping genes (described in Fig. 1E) in 68 ICC cases from an independent cohort containing Caucasian patients (Fig. 3A). Consistently, the 158 overlapping gene signature was significantly associated with patient survival in this cohort ($P < 0.02$) (Fig. 3B). Similar results were obtained when all 636 ICC-specific genes were used for this analysis ($P < 0.04$; Fig. S4).

Integrative Pathway Analysis of ICC-Specific mRNA and MicroRNA. Because microRNA and mRNA are functionally linked, we hypothesized that the expression levels between ICC-specific mRNAs and ICC-specific microRNAs would be highly correlated, as they both are associated with the same stem

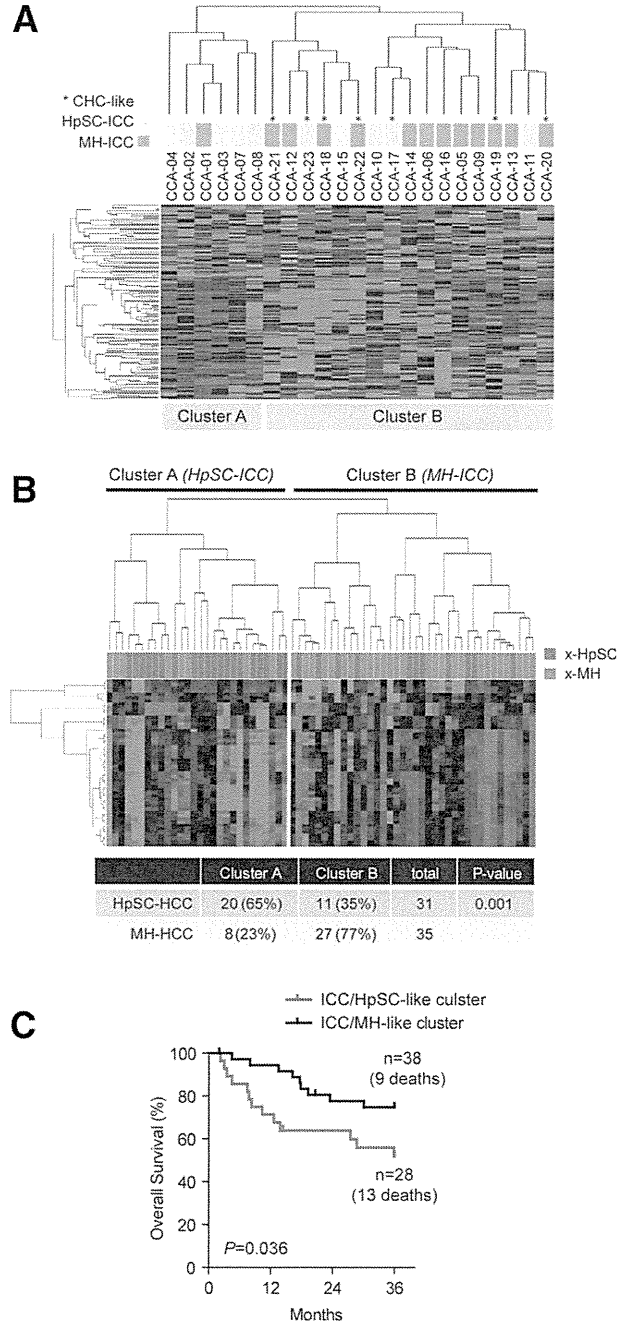

Fig. 2. Heterogeneity of Asian ICC cases revealed by microRNA expression profiling. (A) Unsupervised hierarchical clustering of 23 Asian ICC cases based on global microRNA expression using centered correlation and average linkage. The yellow and light blue bars beneath the dendrogram indicate HpSC-ICC and MH-ICC subgroups, respectively, as classified by mRNA expression profiling described in Fig. 1A. *CHC-like cases. (B) Hierarchical clustering of 61 extreme HCC cases based on the expression of 23 ICC-specific microRNAs. The red and green bars above the heatmap indicate *x*-HpSC and *x*-MH, respectively. A summary of HCC cases based on the dendrogram classification with the ICC-specific signature is included. A chi-squared test was used to determine the correct classification. (C) Kaplan-Meier plot of 61 extreme HCC cases based on the clustering results of (B).

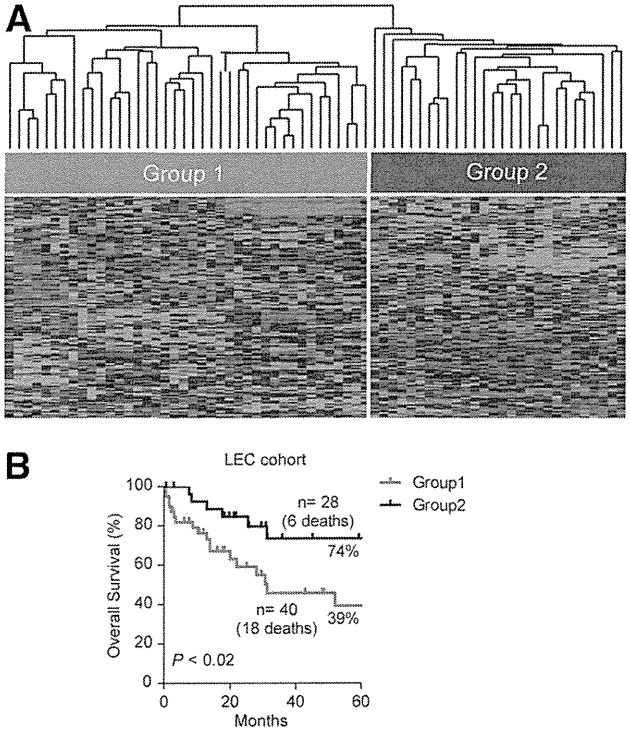

Fig. 3. Validation of the ICC-specific gene signature in an independent ICC cohort as a survival predictor. (A) Hierarchical clustering of 68 Caucasian ICC cases based on the expression of 158 overlapping genes between stem-like ICC and stem-like HCC genes using centered correlation and average linkage. The heatmap depicts high (red) and low (green expression of these genes based on a log2 scale. (B) Kaplan-Meier plot of 68 ICC patients based on the dendrogram classification from (A).

cell-like phenotype. We plotted the density distribution of Spearman correlation coefficients of 636 experimentally derived genes and 23 experimentally derived microRNAs (Fig. 4A). This analysis revealed that there was a clear enrichment of correlative mRNA-microRNA pairs derived from these signatures because a positive correlative curve shifted to the right and a negative correlative curve shifted to the left when compared to a normal distribution curve derived from a global correlation of all available mRNA and microRNA probes (Fig. 4A). A correlation coefficient of 0.5, corresponding to the 95th percentile of the 100-fold random permutations, was used as the cutoff threshold for positive correlation. These results indicated that ICC-specific mRNAs and microRNAs are enriched in the experimentally derived signatures and they are highly correlated.

To determine if there is any enrichment of affected networks associated with ICC subgroups, we combined significantly correlative mRNA-microRNA pairs and performed pathway analysis using Ingenuity Pathway Analysis (IPA, v. 9.0) that incorporates microRNA-mRNA target relationships from TargetScan. Among 1,077 mRNA-microRNA pairs identified by this analysis, 479 pairs showed negative correlation. Among the top nine networks (Table S4), five microRNAs including miR-200c and miR-141 that are encoded by the same transcript were negatively correlated with genes

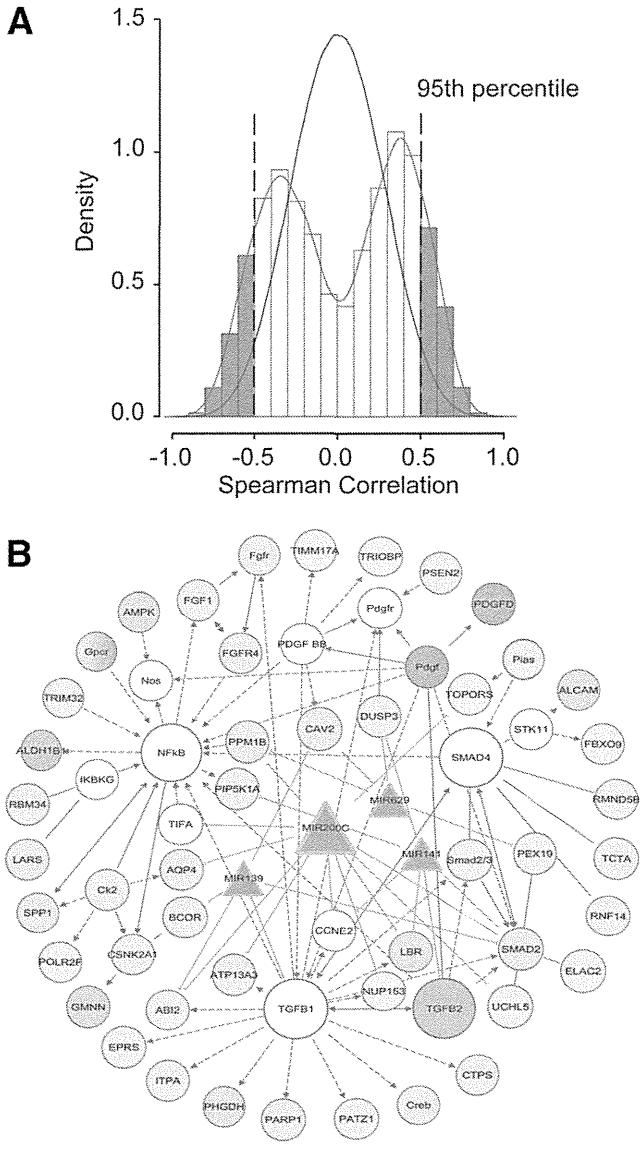

Fig. 4. Integrative analyses of ICC-specific mRNA and microRNAs based on Spearman correlation and ingenuity pathway. (A) Correlation between ICC-specific 636 mRNA and 23 microRNA signatures. (B) The top nine gene networks of signaling including TGF-β, Smad4, and NF-κB pathways activated in stem-like ICC tumors. Red shaded ovals represent up-regulated genes in HpSC-ICC tumors, and open ovals represent genes that are not on the list of significant genes but are reported to be associated with the network. Blue shaded triangles represent down-regulated microRNAs specific to HpSC-ICC tumors. The open ovals that are labeled TGF-β, Smad4, and NF-κB represent molecular nodes related to their respective signaling pathways. Arrows represent positive regulation of gene expression, with solid arrows indicating direct regulation and broken arrows indirect regulation. Blue lines connecting between microRNA and genes represent direct targeting predicted by TargetScan.

in the transforming growth factor beta (TGF-β), nuclear factor kappa B (NF-κB), and Smad signaling pathways (Fig. 4B). A common link between ICC-specific mRNA and microRNA seemed to be related to EMT, where all three pathways are known regulators. Consistently, known stem cell-related genes such as POU5F1 (Oct4), NANOG, NCAM1, and PROM1 (CD133) were much more abundantly expressed in HpSC-ICC than MH-ICC cases (Fig. S5A). TGFB1 was also significantly elevated in HpSC-ICC compared to MH-ICC. However, no difference in EpCAM expression was observed among these two subgroups. An elevated expression of NCAM1 and TGFB1 in a majority of HpSC-ICC cases was confirmed by immonohistochemistry analysis (IHC) (Fig. S5B).

Among the affected networks, it was noticeable that miR-200c appeared a common molecular note linking to EMT, as it had a direct interaction with many of the affected genes in this pathway (Fig. 4B). Consistently, the expression level of miR-200c was associated with overall survival and disease-free survival in ICC cases (Fig. S6). These data suggested that miR-200c may play an important role in maintaining HpSC-like phenotype.

To determine whether EMT was functionally linked to HpSC-ICC cells, we first analyzed representative expression levels of EMT markers in ICC specimens by qRT-PCR. Consistently, mesenchymal markers such as ZEB1, ZEB2, CDH2, and VIM were more abundantly expressed, whereas an epithelial marker, CDH1, and miR-141/miR-200c were much less abundantly expressed in HpSC-ICC cases as compared to MH-ICC cases (Fig. 5A). Next, we determined if an altered miR-200c expression could lead to EMT in ICC cells. We selected two ICC cell lines that represent two opposite ends of the EMT spectrum. A nonmalignant H69 cell line derived from normal human intrahepatic cholangiocytes was included as a control.[24] HuH28 cells had fibroblast-like cell morphology with mesenchymal appearances and expressed very low levels of miR-200c but high levels of mesenchymal markers, whereas HuCCT1 cells had cobblestone-like cell morphology with epithelial appearances and expressed high levels of miR-200c but low levels of mesenchymal markers (Fig. 5B). The miR-200c level was also relatively high in H69 cells with epithelial morphology. Transient transfection of miR-200c oligos in HuH28 cells induced a reversed EMT from a mesenchymal-like to a cobblestone-like morphology with a suppression of genes that mediate EMT (Fig. 5C). Conversely, transfection of an anti-miR-200c oligo in HuCCT1 resulted in an induction of mesenchymal markers (Fig. 5D). In addition, overexpression of miR-200c suppressed cell migration (Fig. 5E) and invasion (Fig. 5F) in HuH28 cells. However, miR-200c did not affect cell proliferation and apoptosis in HUH28 cells as measured by 3-(4,5-dimethylthiazol-2-yl)-2,5-diphenyltetrazolium bromide (MTT) and Transferase-Mediated dUTP Nick-End Labeling (TUNEL) assays (Fig. S7).

Analyses of the genomic region encoding the human miR-200c/miR-141 locus at the UCSC Genome Browser revealed that miR-200c and miR-141 are derived from a single transcript encoded by a predicted gene (ENST00000537269) (Fig. 6A). The available Chip-Seq data revealed several transcriptional factors such as c-Myc and TCF4 to be preferentially bound to the immediate 5′ upstream sequence of the predictive transcription initiation site. To determine whether c-myc directly regulates miR-200c expression, we silenced c-Myc expression with a c-myc-specific small interfering RNA (siRNA) in HuH28 cells and examined the activity of a luciferase reporter containing an upstream 0.9 kb fragment of pri-miR-200c[25] (Fig. 6B). Consistently, we found that inhibition of c-Myc resulted in an increased hmiR-200cLuc activity. Moreover, c-myc siRNA could effectively induce endogenous miR-200c expression, however suppress mesenchymal markers but induce epithelial marker (Fig. 6C).

NCAM1 as a Direct Target of MiR-200c. Because several stem/progenitor cell-related genes such as POU5F1, NANOG, MYC, TGFB1, NCAM1, and PROM1 are overexpressed in HpSC-ICC cases (Fig. S5), we reasoned that some of these genes may be targets of miR-200c. TargetScan analysis (TargetScanHuman 6.0) revealed that only NCAM1 contained a classical and evolutionarily conserved miR-200c binding site at its 3′ untranslated region (UTR) (Fig. 7A). Ectopic expression of miR-200c in HuH28 cells resulted in a reduction (Fig. 7B), whereas inhibition of miR-200c in HuCCT1 cells led to an increased expression of NCAM1 (Fig. 7C). To further determine whether NCAM1 was a bona fide target of miR-200c-mediated silencing, the miR-200c binding site was cloned into a luciferase reporter. We found that forced expression of miR-200c in HUH28 cells resulted in decreased luciferase activity when a wildtype sequence but not a mutant sequence was present (Fig. 7D). Moreover, inhibition of miR-200c in HuCCT1 cells resulted in increased luciferase activity only from a wildtype reporter (Fig. 7E). Consistently, ICC cases with high levels of NCAM1 had a worse survival compared to those with low NCAM1 expression (Fig. 7F). Moreover, a significant inverse correlation was observed between miR-200c and NCAM1 (Fig. 7G).

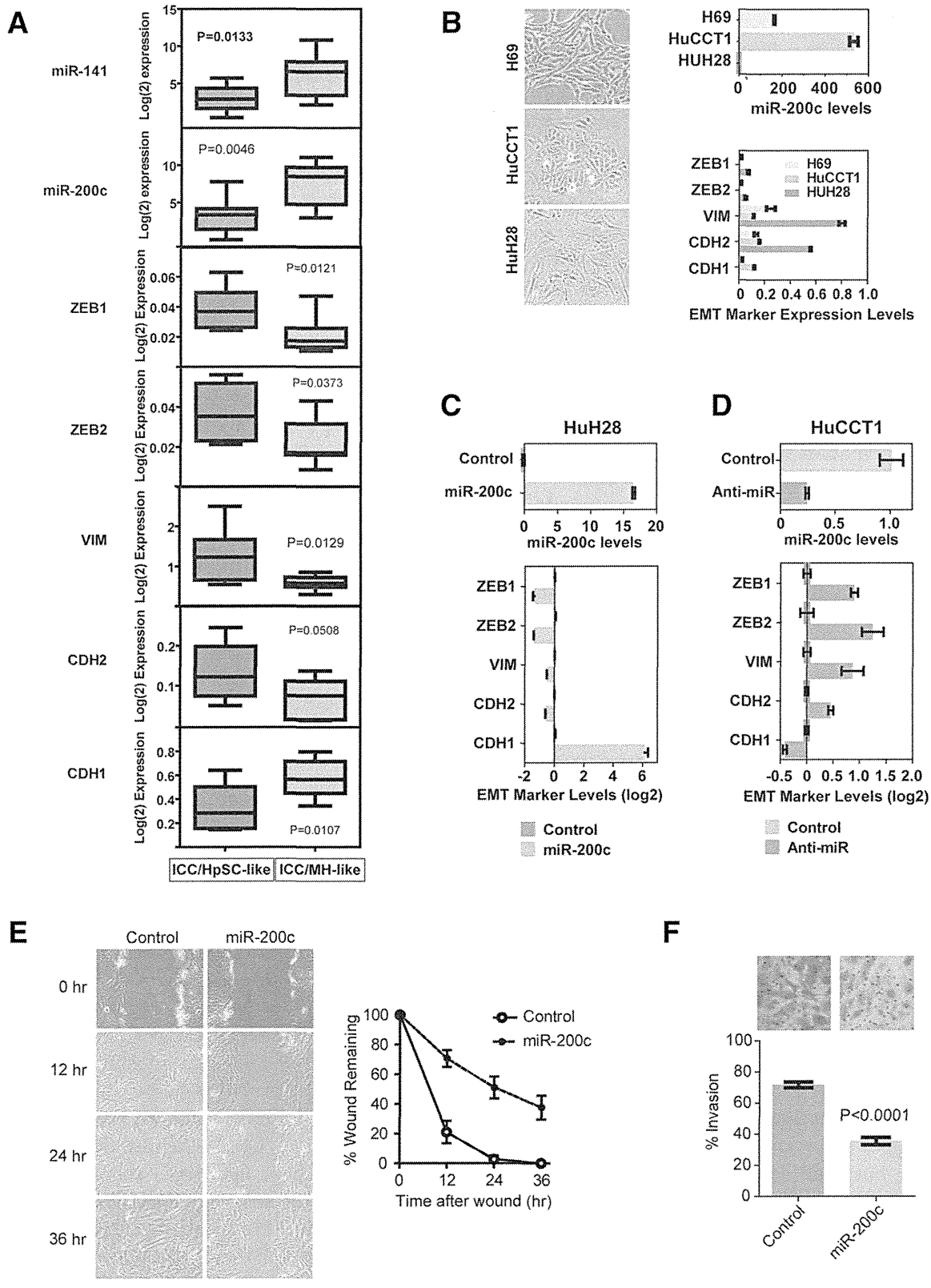

Fig. 5. Inactivation of miR-200c/miR-141 and activation of EMT-related genes are associated with stem-like ICC. (A) Expression analyses of miR-141/miR-200c transcripts and EMT-specific markers based qRT-PCR data in eight HpSC-ICC and eight MH-ICC samples classified by gene clustering from Fig. 1. The horizontal lines in the boxplots represent the median, the boxes represent the interquartile range, and the whiskers represent the 10th and 90th percentiles. A nonparametric test was used to compare the two groups and *P* values are indicated. (B) Expression of miR-200c and EMT-specific genes in HuH28, HuCCT1, and H69 cells as analyzed by qRT-PCR. (C) Expression of EMT-specific genes in HuH28 cells transduced with miR-200c as analyzed by qRT-PCR. (D) Expression of EMT-specific genes in HuCCT1 cells transduced with an anti-miR-200c oligo as analyzed by qRT-PCR. (E) Cell migration of HuH28 cells transduced with miR-200c as determined by the wound healing assay. (F) Cell invasion of HuH28 cells transduced with miR-200c as determined by the Boyden chamber cell invasion assay. Representative images are shown.

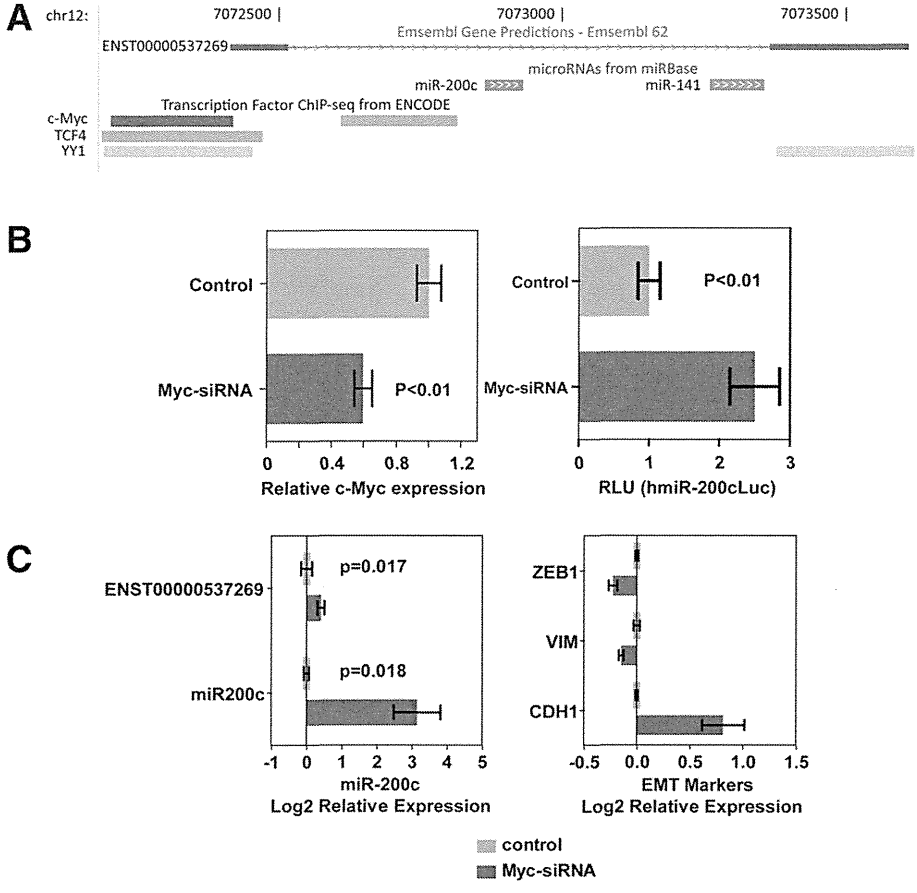

Fig. 6. c-Myc-mediated silencing of miR-200c and induction of EMT. (A) The genome position of ENST00000537269 encoding miR-200c and miR-141, based on Ensembl Gene Predictions using UCSC Genome Browser. (B) Effect of c-Myc siRNA on miR-200cc-Myc expression (left panel) and the miR-200c promoter luciferase activity (right panel) in HuCCT1 cells. (C) Effect of c-Myc siRNA on endogenous levels of miR-200c and induction of EMT-related gene expression in HuCCT1 cells.

Discussion

Similar to HCC, ICC is heterogeneous in clinical presentation, although our knowledge related to its tumor biology is limited. Several recent studies have begun dissecting the molecular pathogenesis of ICC including functional roles of microRNA in ICC cells.[27,28] Recently, we used global transcriptomic approaches to study HCC heterogeneity and identified critical genetic loci functionally linked to hepatic CSCs with gene expression profiles resembling normal hepatic stem cells.[7,8] We also used these approaches to study cholangiocarcinoma.[15,23] In this study, we examined whether ICC and HCC are distinct at the transcriptomic levels. Using two independent transcriptomics approaches, we found that ICC cases from Asian patients can be mainly divided into two subgroups with one resembling of stem-like HCC and other mature hepatocyte-like HCC. Consistently, we found that several known hepatic stem/progenitor cell-specific genes such as POU5F1 (Oct4), NANOG, MYC, TGFB1, NCAM1, and PROM1 are more abundantly expressed in stem-like ICC than mature hepatocyte-like ICC.[29] Moreover, both ICC-specific mRNA and microRNA signatures could independently predict HCC survival as well as ICC prognosis in Caucasian patients. These results are consistent with our recent finding that a subset of HCC may share an ICC-like gene expression trait.[15] Integrative pathway analyses revealed that an altered miR-200c signaling pathway linked to EMT may be responsible for the maintenance of stem-like ICC associated with poor prognosis. For example, we found that two significant microRNAs, i.e., miR-200c and miR-141, encoded by the same transcript, were negatively correlated with genes in the TGF-β, NF-κB, and Smad signaling pathways. These two microRNAs share the same seed sequences and are predicted to have similar cellular functions. EMT is an important biological process contributing to embryogenesis and organ development.[30] Recently, components of EMT have been shown to be critical in promoting cancer invasion and metastasis.[31] TGF-β is essential for the induction of EMT during various stages of embryogenesis and plays an important role in carcinoma progression into an invasive state.[32-34] Smad signaling is essential for TGF-β-induced EMT.[35] Furthermore, miR-200 family members including miR-141 and miR-200c induce epithelial differentiation, thereby suppressing EMT by inhibiting translation of mRNA for the EMT-activators ZEB1 and

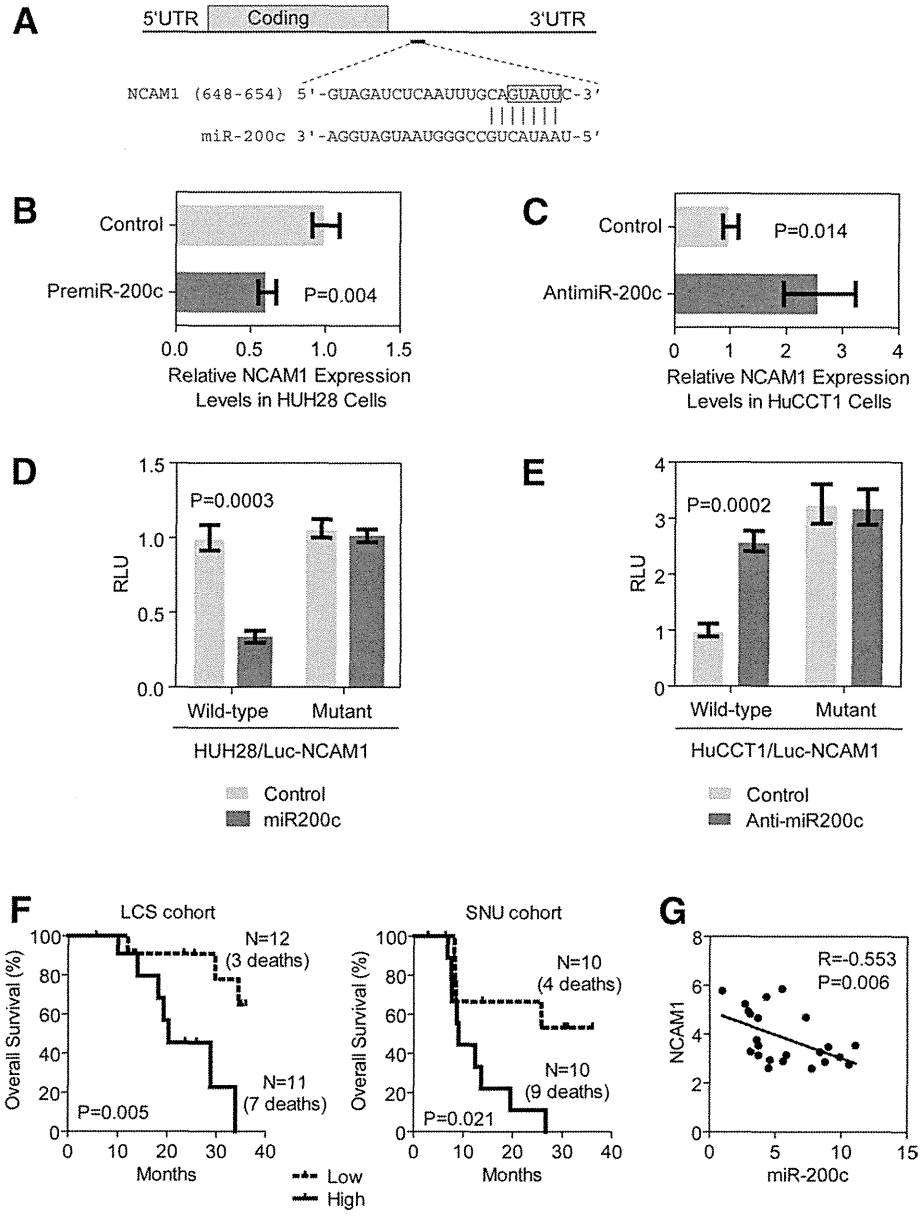

Fig. 7. Functional interactions between miR-200c and NCAM1. (A) Predicted duplex formation between the 3′UTR sequences of human NCAM1 and miR-200c where vertical bars represent the paired seed sequences. The box highlights the nucleotides that were changed to CAUAA in a mutant luciferase reporter. (B) Effect of premiR-200c oligo on NCAM1 expression in HuH28 cells as determined by qRT-PCR. (C) Effect of anti-miR-200c oligo on NCAM1 expression in HuCCT1 cells as determined by qRT-PCR. (D) Luciferase activities of wild-type and mutant reporters in HuH28 cells with or without the presence of pre-miR-200c oligo. (E) Luciferase activities of wildtype and mutant reporters in HuCCT1 cells with or without the presence of anti-miR200c oligo. Each experiment was repeated at least three times and the expression value is shown as the mean ± standard deviation. (F) Kaplan-Meier estimates of overall survival according to expression of NCAM1 in ICC cases from LCS and SNU cohorts. NCAM1 expression values were dichotomized into low and high groups using the within cohort median expression value as a cutoff. (G) Spearman correlation analysis of NCAM1 and miR-200c expression data as determined by mRNA and microRNA arrays.

ZEB2.[36,37] miR-200 family members are functionally linked to EMT, in part by way of targeting ZEB1 and ZEB2, as well as cell migration, invasion, and tumorigenicity.[36,38] These results suggest that the ZEB1-miR-200 feedback loop is critical for maintaining aggressive tumor features. In addition, we also found that miR-200c directly targets NCAM1. NCAM1 is highly expressed in hepatic stem cells and its function has been tightly linked to EMT.[29,39] Our results are consistent with the hypothesis that the miR-200-EMT gene axis may be functional critical to the development of stem-like ICC. Shared molecular activities including EMT and microRNA among HCC and ICC have been noted in recent publications.[40,41] Interestingly, abnormal regulation of EMT-related genes has been reported to be linked to HCC development.[42-44] However, no evidence has linked miR-200 to HCC development. Consistently, we found no evidence that miR-200c is silenced in stem-like HCC (data not shown). It is plausible that the miR-200c-EMT gene axis is a unique signaling pathway functionally important for stem-like ICC and could be exploited as molecular targets for ICC therapies. In addition, unlike HCC, EpCAM is not a good prognostic biomarker for ICC because its expression is highly elevated in both HpSC-ICC and MH-ICC (data not shown). Further studies involving in-depth analyses of miR-200c and EMT signaling and using relevant animal models would be needed to test the therapeutic relevance of these targets for ICC.

Human adult livers are believed to be comprised of maturational lineages of cells beginning intrahepatically

near the portal triads referred to as canals of Hering.[45] This region is close to intrahepatic bile ducts and is believed to contain liver stem cells. It is suggested that liver stem cells may give rise to bipotent progenitor cells, which have the potential to differentiate into both hepatocytic and cholangiocytic lineages. In principle, hepatic stem/progenitor cells could be the common cellular origin for both HCC and ICC. It is hypothesized that cancer progression is driven by the presence of CSC, which is also responsible for treatment resistance and tumor relapse.[46] CSCs have been demonstrated in a growing range of epithelial and other solid organ malignancies, suggesting that the majority of malignancies are dependent on such a compartment.[47] This model is attractive because it may help to address the heterogeneity of HCC and ICC, and could facilitate research strategies to define novel and effective therapies.[48] Consistently, studies on clinicopathological features of ICC suggest that some ICCs could arise from liver stem cells rather than from mature cholangiocytes.[49,50] Moreover, gene expression profiling revealed that some HCC cases contain ICC-like gene expression trait and embryonic stem cell-like traits.[15] These results suggest that certain types of ICC could be derived from the same cell origin that leads to HCC, whereas distinct mechanisms may be involved in the genesis of ICC.

CHC has been traditionally classified into three subtypes based on the histological description by Allen and Lisa in 1949.[51] These subtypes include type-A (collision or double cancer, which is referred to as separate HCC and ICC arising in the same liver), type-B (contiguous mass, which is referred to as admixed HCC/ICC such as fibrolamellar tumors), and type-C (transitional tumors, which are referred to as a tumor mass with cellular features of both HCC and ICC). In type-A tumors, the HCC and ICC lesions could be interpreted as originating separately from hepatocyte and bile duct epithelium. Type-B tumors could follow the same mechanism as type-A because it is difficult to distinguish them based on histological data. Because both HCC and ICC cellular features are intimately associated with the type-C tumors, they have been interpreted as arising from the same site and sharing the same cell origin. In our study, two Chinese and five Japanese CHC cases belong to type-B and seven Korean CHC cases[15] belong to type-C. Hierarchical clustering analyses revealed that both type-B and type-C CHC samples could be divided into stem-like ICC and mature hepatocyte-like ICC, which are also associated with survival (Fig. S8). Although these results are not conclusive due to limited cases, they appear consistent with the hypothesis that both type-B and type-C CHC could originate from the same hepatic progenitor cells shared by HCC and CHC tumors. A new histological subtyping of CHC according to the WHO Classification based on the presence of stem-cell features has been proposed.[52] Long-term follow-up of larger cohorts is needed to define the clinical and biological behavior of all CHC cases.

Our analysis dissecting the heterogeneous ICC based on the expression of stem cell-like signatures could classify ICC cases into subgroups with more uniform and prognostic phenotypes. In principle, targeting molecular pathways specific to each subpopulation would be more effective for the development of personalized clinical strategies. We suggest that the miR-200c-associated EMT pathway and stem-cell activities may contribute to the development of the HpSC-ICC tumors. The association of EMT with poor prognosis is well known in many cancer types. Moreover, recent studies have demonstrated the critical role of miR200c in the control of stem/progenitor cell renewal and differentiation. Our findings are consistent with the hypothesis supporting the pivotal role of miR-200c in the aggressive progression of stem-like ICC.

Acknowledgment: We thank Drs. Gregory J. Gores for H69 cells, Kathleen C. Flanders and Lalage M. Wakefield for anti-TGF-beta1 antibody, and Li Wang for the miR-200c luciferase reporter. We also thank Dr. Xiaolin Wu and members of the microarray core at the NCI-SAIC for help on microarray analysis and Ms. Karen Yarrick for bibliographic assistance.

References

1. Jemal A, Bray F, Center MM, Ferlay J, Ward E, Forman D.Global cancer statistics. CA Cancer J Clin 2011;61:69-90.
2. Martin R, Jarnagin W.Intrahepatic cholangiocarcinoma. Current management. Minerva Chir 2003;58:469-478.
3. Shaib Y, El-Serag HB.The epidemiology of cholangiocarcinoma. Semin Liver Dis 2004;24:115-125.
4. Berthiaume EP, Wands J.The molecular pathogenesis of cholangiocarcinoma. Semin Liver Dis 2004;24:127-137.
5. Komuta M, Spee B, Vander BS, De VR, Verslype C, Aerts R, et al. Clinicopathological study on cholangiolocellular carcinoma suggesting hepatic progenitor cell origin. HEPATOLOGY 2008;47:1544-1556.
6. Zhou H, Wang H, Zhou D, Wang H, Wang Q, Zou S, et al. Hepatitis B virus-associated intrahepatic cholangiocarcinoma and hepatocellular carcinoma may hold common disease process for carcinogenesis. Eur J Cancer 2010;46:1056-1061.
7. Lee JS, Heo J, Libbrecht L, Chu IS, Kaposi-Novak P, Calvisi DF, et al. A novel prognostic subtype of human hepatocellular carcinoma derived from hepatic progenitor cells. Nat Med 2006;12:410-416.
8. Yamashita T, Ji J, Budhu A, Forgues M, Yang W, Wang HY, et al. EpCAM-positive hepatocellular carcinoma cells are tumor-initiating cells with stem/progenitor cell features. Gastroenterology 2009;136:1012-1024.
9. Yamashita T, Forgues M, Wang W, Kim JW, Ye Q, Jia H, et al. EpCAM and alpha-fetoprotein expression defines novel prognostic subtypes of hepatocellular carcinoma. Cancer Res 2008;68:1451-1461.

10. Cairo S, Wang Y, de RA, Duroure K, Dahan J, Redon MJ, et al. Stem cell-like micro-RNA signature driven by Myc in aggressive liver cancer. Proc Natl Acad Sci U S A 2010;107:20471-20476.
11. Ma S, Chan KW, Hu L, Lee TK, Wo JY, Ng IO, et al. Identification and characterization of tumorigenic liver cancer stem/progenitor cells. Gastroenterology 2007;132:2542-2556.
12. Yang ZF, Ho DW, Ng MN, Lau CK, Yu WC, Ngai P, et al. Significance of CD90(+) cancer stem cells in human liver cancer. Cancer Cell 2008;13:153-166.
13. Haraguchi N, Ishii H, Mimori K, Tanaka F, Ohkuma M, Kim HM, et al. CD13 is a therapeutic target in human liver cancer stem cells. J Clin Invest 2010;120:3326-3339.
14. Tang Y, Kitisin K, Jogunoori W, Li C, Deng CX, Mueller SC, et al. Progenitor/stem cells give rise to liver cancer due to aberrant TGF-beta and IL-6 signaling. Proc Natl Acad Sci U S A 2008;105:2445-2450.
15. Woo HG, Lee JH, Yoon JH, Kim CY, Lee HS, Jang JJ, et al. Identification of a cholangiocarcinoma-like gene expression trait in hepatocellular carcinoma. Cancer Res 2010;70:3034-3041.
16. Budhu A, Forgues M, Ye QH, Jia LH, He P, Zanetti KA, et al. Prediction of venous metastases, recurrence and prognosis in hepatocellular carcinoma based on a unique immune response signature of the liver microenvironment. Cancer Cell 2006;10:99-111.
17. Budhu A, Jia HL, Forgues M, Liu CG, Goldstein D, Lam A, et al. Identification of metastasis-related microRNAs in hepatocellular carcinoma. HEPATOLOGY 2008;47:897-907.
18. Ji J, Yamashita T, Budhu A, Forgues M, Jia HL, Li C, et al. Identification of microRNA-181 by genome-wide screening as a critical player in EpCAM-positive hepatic cancer stem cells. HEPATOLOGY 2009;50:472-480.
19. Ji J, Shi J, Budhu A, Yu Z, Forgues M, Roessler S, et al. MicroRNA expression, survival, and response to interferon in liver cancer. N Engl J Med 2009;361:1437-1447.
20. Ye QH, Qin LX, Forgues M, He P, Kim JW, Peng AC, et al. Predicting hepatitis B virus-positive metastatic hepatocellular carcinomas using gene expression profiling and supervised machine learning. Nat Med 2003;9:416-423.
21. Woo HG, Wang XW, Budhu A, Kim YH, Kwon SM, Tang ZY, et al. Association of TP53 mutations with stem cell-like gene expression and survival of patients with hepatocellular carcinoma. Gastroenterology 2011;140:1063-1070.e8.
22. Woo HG, Park ES, Lee JS, Lee YH, Ishikawa T, Kim YJ, et al. Identification of potential driver genes in human liver carcinoma by genome-wide screening. Cancer Res 2009;69:4059-4066.
23. Andersen JB, Spee B, Blechacz BR, Avital I, Komuta M, Barbour A, et al. Genomic and genetic characterization of cholangiocarcinoma identifies therapeutic targets for tyrosine kinase inhibitors. Gastroenterology 2012;142:1021-1031.
24. Park J, Gores GJ, Patel T. Lipopolysaccharide induces cholangiocyte proliferation via an interleukin-6-mediated activation of p44/p42 mitogen-activated protein kinase. HEPATOLOGY 1999;29:1037-1043.
25. Zhang Y, Yang Z, Whitby R, Wang L.Regulation of miR-200c by nuclear receptors PPARalpha, LRH-1 and SHP. Biochem Biophys Res Commun 2011;416:135-139.
26. Roessler S, Jia HL, Budhu A, Forgues M, Ye QH, Lee JS, et al. A unique metastasis gene signature enables prediction of tumor relapse in early-stage hepatocellular carcinoma patients. Cancer Res 2010;70:10202-10212.
27. Meng F, Henson R, Lang M, Wehbe H, Maheshwari S, Mendell JT, et al. Involvement of human micro-RNA in growth and response to chemotherapy in human cholangiocarcinoma cell lines. Gastroenterology 2006;130:2113-2129.
28. Mott JL, Kobayashi S, Bronk SF, Gores GJ.mir-29 regulates Mcl-1 protein expression and apoptosis. Oncogene 2007;26:6133-6140.
29. Turner R, Lozoya O, Wang Y, Cardinale V, Gaudio E, Alpini G, et al. Human hepatic stem cell and maturational liver lineage biology. HEPATOLOGY 2011;53:1035-1045.
30. Kalluri R, Weinberg RA.The basics of epithelial-mesenchymal transition. J Clin Invest 2009;119:1420-1428.
31. Yang J, Mani SA, Donaher JL, Ramaswamy S, Itzykson RA, Come C, et al. Twist, a master regulator of morphogenesis, plays an essential role in tumor metastasis. Cell 2004;117:927-939.
32. Oft M, Heider KH, Beug H.TGFbeta signaling is necessary for carcinoma cell invasiveness and metastasis. Curr Biol 1998;8:1243-1252.
33. Heldin CH, Landstrom M, Moustakas A.Mechanism of TGF-beta signaling to growth arrest, apoptosis, and epithelial-mesenchymal transition. Curr Opin Cell Biol 2009;21:166-176.
34. Nawshad A, Lagamba D, Polad A, Hay ED.Transforming growth factor-beta signaling during epithelial-mesenchymal transformation: implications for embryogenesis and tumor metastasis. Cells Tissues Organs 2005;179:11-23.
35. Pardali K, Moustakas A.Actions of TGF-beta as tumor suppressor and pro-metastatic factor in human cancer. Biochim Biophys Acta 2007;1775:21-62.
36. Burk U, Schubert J, Wellner U, Schmalhofer O, Vincan E, Spaderna S, et al. A reciprocal repression between ZEB1 and members of the miR-200 family promotes EMT and invasion in cancer cells. EMBO Rep 2008;9:582-589.
37. Park SM, Gaur AB, Lengyel E, Peter ME.The miR-200 family determines the epithelial phenotype of cancer cells by targeting the E-cadherin repressors ZEB1 and ZEB2. Genes Dev 2008;22:894-907.
38. Wellner U, Schubert J, Burk UC, Schmalhofer O, Zhu F, Sonntag A, et al. The EMT-activator ZEB1 promotes tumorigenicity by repressing stemness-inhibiting microRNAs. Nat Cell Biol 2009;11:1487-1495.
39. Frame MC, Inman GJ.NCAM is at the heart of reciprocal regulation of E-cadherin- and integrin-mediated adhesions via signaling modulation. Dev Cell 2008;15:494-496.
40. Seok JY, Na DC, Woo HG, Roncalli M, Kwon SM, Yoo JE, et al. A fibrous stromal component in hepatocellular carcinoma reveals a cholangiocarcinoma-like gene expression trait and EMT. HEPATOLOGY 2012;55:1776-1786.
41. Meng F, Glaser SS, Francis H, DeMorrow S, Han Y, Passarini JD, et al. Functional analysis of microRNAs in human hepatocellular cancer stem cells. J Cell Mol Med 2012;16:160-173.
42. Giannelli G, Bergamini C, Fransvea E, Sgarra C, Antonaci S.Laminin-5 with transforming growth factor-beta1 induces epithelial to mesenchymal transition in hepatocellular carcinoma. Gastroenterology 2005;129:1375-1383.
43. Lee TK, Poon RT, Yuen AP, Ling MT, Kwok WK, Wang XH, et al. Twist overexpression correlates with hepatocellular carcinoma metastasis through induction of epithelial-mesenchymal transition. Clin Cancer Res 2006;12:5369-5376.
44. Jou J, Diehl AM.Epithelial-mesenchymal transitions and hepatocarcinogenesis. J Clin Invest 2010;120:1031-1034.
45. Sigal SH, Brill S, Fiorino AS, Reid LM. The liver as a stem cell and lineage system. Am J Physiol 1992;263:G139-G148.
46. Clevers H.The cancer stem cell: premises, promises and challenges. Nat Med 2011;17:313-319.
47. Alison MR, Islam S, Wright NA. Stem cells in cancer: instigators and propagators? J Cell Sci 2010;123:2357-2368.
48. Oishi N, Wang XW.Novel therapeutic strategies for targeting liver cancer stem cells. Int J Biol Sci 2011;7:517-535.
49. Lee JH, Rim HJ, Sell S.Heterogeneity of the "oval-cell" response in the hamster liver during cholangiocarcinogenesis following Clonorchis sinensis infection and dimethylnitrosamine treatment. J Hepatol 1997;26:1313-1323.
50. Ishii T, Yasuchika K, Suemori H, Nakatsuji N, Ikai I, Uemoto S.Alpha-fetoprotein producing cells act as cancer progenitor cells in human cholangiocarcinoma. Cancer Lett 2010;294:25-34.
51. Allen RA, Lisa JR.Combined liver cell and bile duct carcinoma. Am J Pathol 1949;25:647-655.
52. Theise ND, Nakashima O, Park YN, Nakanuma Y. Combined hepatocellular-cholangiocarcinoma. In: Bosman FT, Carneiro F, Hruban RH, Theise ND, editors. WHO classification of tumours of the digestive system. Lyon, France: World Health Organization; 2010:225-227.

STEM CELLS AND DEVELOPMENT
Volume 21, Number 16, 2012
© Mary Ann Liebert, Inc.
DOI: 10.1089/scd.2011.0725

Nucleostemin in Injury-Induced Liver Regeneration

Haruhiko Shugo,[1,2,*] Takako Ooshio,[1,*] Masako Naito,[1] Kazuhito Naka,[1] Takayuki Hoshii,[1] Yuko Tadokoro,[1] Teruyuki Muraguchi,[1] Akira Tamase,[1] Noriyuki Uema,[1] Taro Yamashita,[2] Yasunari Nakamoto,[2] Toshio Suda,[3] Shuichi Kaneko,[2] and Atsushi Hirao[1]

The high regenerative capacity of liver contributes to the maintenance of its size and function when injury occurs. Partial hepatectomy induces division of mature hepatocytes to maintain liver function, whereas severe injury stimulates expansion of undifferentiated hepatic precursor cells, which supply mature cells. Although several factors reportedly function in liver regeneration, the precise mechanisms underlying regeneration remain unclear. In this study, we analyzed expression of nucleostemin (NS) during development and in injured liver by using transgenic green fluorescent protein reporter (NS-GFP Tg) mice. In neonatal liver, the hepatic precursor cells that give rise to mature hepatocytes were enriched in a cell population expressing high levels of NS. In adult liver, NS was abundantly expressed in mature hepatocytes and rapidly upregulated by partial hepatectomy. Severe liver injury promoted by a diet containing 3,5-diethoxycarbonyl-1,4-dihydrocollidine induced the emergence of NS-expressing ductal epithelial cells as hepatic precursor cells. NS knockdown inhibited both hepatic colony formation in vitro and proliferation of hepatocytes in vivo. These data strongly suggest that NS plays a critical role in regeneration of both hepatic precursor cells and hepatocytes in response to liver injury.

Introduction

The liver is an organ with high regenerative capacity, enabling it to maintain a constant size and function following injury [1,2]. In resting liver, hepatocytes are quiescent and rarely undergo cell division. Therefore, hepatocyte replacement occurs slowly in static conditions. However, when the liver is injured, cells replicate to restore loss of tissue mass and function. Proliferation of hepatocytes and bile duct epithelial cells contributes to liver maintenance. After partial hepatectomy, the remaining lobes regenerate the entire liver mass within 5–7 days, a process accomplished primarily by division of mature cells rather than of stem/precursor cells. In mice, division of hepatocytes starts after partial hepatectomy and is maximal 24–48 h later. Several molecules, including hepatocyte growth factor (HGF), interleukin-6, tumor necrosis factor α, transforming growth factor, and epidermal growth factor (EGF), reportedly govern this process [1,2]. Termination of regeneration is also important for the maintenance of homeostasis. In severe injury associated with defects in hepatocyte proliferation, it is believed that bipotential precursors of hepatocytes and cholangiocytes contribute to liver regeneration [3,4]. Currently, it is thought that potential hepatic precursor cells emerge from smaller branches of the biliary tree. In rats, a population of small cells exhibiting large nuclei, called oval cells, emerges around portal veins following liver injury [5]. In mice, a diet supplemented with 3,5-diethoxycarbonyl-1,4-dihydrocollidine (DDC) induces ductal proliferation and morphological changes similar to those seen in the rat oval cell response [6]. Precursor cells appear to regenerate hepatocytes and cholangiocytes through proliferation, migration, and differentiation processes. Thus, proper control of both mature cells and hepatic stem/precursor cells is critical for liver regeneration.

Nucleostemin (NS) is a GTPase that binds to p53 and was originally reported to be highly expressed in stem cells from several tissues, including embryonic stem (ES) cells, immature hematopoietic cells, and neural stem/progenitor cells [7]. NS loss results in reduced cell proliferation and increased apoptosis in both ES cells and ES cell-derived neural stem/progenitor cells [8]. Structural comparisons have been used to isolate NS homologues in *Caenorhabditis elegans* [9], newt [10], *Xenopus* [11], mouse [7], and human [12]. In the regenerating newt lens, NS protein rapidly accumulates in nucleoli of dedifferentiating pigmented epithelial cells and multinucleate muscle fibers [10], suggesting that its expression correlates with undifferentiated status in newt cells. In contrast, the NS homologue in *Caenorhabditis elegans* (*nst-1*) is expressed in both proliferating and differentiated cells. *Nst-1* mutants exhibit defects in larval growth and cell cycle

[1]Division of Molecular Genetics, Cancer Research Institute, Kanazawa University, Kanazawa, Japan.
[2]Disease Control and Homeostasis, Kanazawa University Graduate School of Medical Science, Kanazawa, Japan.
[3]Department of Cell Differentiation, The Sakaguchi Laboratory of Developmental Biology, Keio University School of Medicine, Tokyo, Japan.
*These authors contributed equally to this work.

progression in germline stem cells [9]. Because *nst-1*-mutant germ cells can still differentiate into mature sperm, nst-1 may play a critical role in germline stem cell proliferation but not in differentiation. In addition, NS is reportedly expressed at similar levels in non-proliferating muscle stem cells (satellite cells), rapidly proliferating precursor cells (myoblasts), and post-mitotic terminally differentiated cells (myotubes and myofibers) [13]. NS downregulation inhibits differentiation of myoblasts to myotubes, suggesting a role in post-mitotic terminal differentiation in this type. Thus, NS has pleiotropic effects on cellular function, and it is unclear how NS is involved in cell differentiation.

In a previous study, we generated a reporter system where the NS promoter drives green fluorescent protein (GFP) expression (termed NS-GFP) in vivo [14]. We successfully used this reporter system to identify a specific fraction of neonatal germ cells as spermatogonial stem cells with long-term repopulating capacity. We also combined the NS reporter system with a mouse brain tumor model and demonstrated the existence of an undifferentiated tumor-initiating cell (TIC) population in a highly aggressive brain tumor by analyzing GFP fluorescence intensity [15]. Consistent with our data, a recent report employing a bacterial artificial chromosome transgenic mouse line expressing GFP from the NS promoter showed that NS-enriched mammary tumor cells are highly tumorigenic in vitro and in vivo [16]. Further, another recent report showed that NS overexpression enhanced tumorigenicity of TICs, increased expression of genes that maintain undifferentiated status, and enhanced radioresistance [17]. These data suggest that NS functions to maintain stem cell properties in malignant cells.

In this study, we examined the expression and function of NS in liver. Interestingly, we found that NS contributes to the proliferation of hepatocytes after partial hepatectomy and to the regenerative capacity of hepatic precursor cells. Our data strongly suggest that NS is essential for injury-induced liver regeneration.

Materials and Methods

Animals

Mice used in this study were on a C57BL/6 background. NS-GFP Tg mice were generated as described previously [14]. Livers were collected at fetal (embryonic day 14.5: E14.5), neonatal (postnatal day 5: P5), and adult (8 weeks old) stages. For experiments involving severe liver injury, adult mice were fed a diet containing 0.1% DDC (Sigma-Aldrich, St. Louis, MO) for 2 weeks [6]. For partial hepatectomy, mice were anesthetized and 70% of the liver was resected. All procedures were performed in accordance with the animal care guidelines of Kanazawa University.

Isolation of liver cells

For digestion of fetal or neonatal liver cells, livers were minced and dissociated with enzyme-based dissociation buffer (Invitrogen Life Technologies, Carlsbad, CA) as described previously [18]. For isolation of adult liver cells, a 2-step perfusion method was utilized [19]. Briefly, perfusion collagenase solution (0.5 g/L; Sigma-Aldrich) was administered to a sacrificed mouse via the portal vein. Nonparenchymal cells were separated from parenchymal cells by centrifugation (50 *g*, 1 min), and dead cells were removed by centrifugation through 25% Percoll solution (GE Healthcare, Tokyo, Japan).

Flow cytometry

Single-cell suspensions from fetal, neonatal, or adult liver were incubated with an anti-CD16/CD32 antibody on ice for 10 min, followed by incubation with phycoerythrin (PE)-conjugated anti-TER119 and anti-CD45 antibodies (BD Pharmingen, San Diego, CA) on ice for 30 min. Cells were washed thrice in staining solution [2% fetal calf serum (FCS)/phosphate-buffered saline (PBS)] and incubated with anti-PE microbeads (Miltenyi Biotech, Bergisch Gladbach, Germany). After 3 washes, $CD45^-TER119^-$cells were collected (MACS; Miltenyi Biotech). Fetal liver cells were incubated with a biotin-conjugated anti-Dlk antibody (MBL, Nagoya, Japan), followed by incubation with allophycocyanin-conjugated streptavidin antibody (BD Pharmingen). Dead cells were stained with propidium iodide. Fluorescence-labeled cells were analyzed and sorted with JSAN (Bay Bioscience Co, Kobe, Japan).

Hepatic colony forming assay

Cells fractionated by flow cytometry were inoculated at 2,500 cells/well into six-well dishes coated with type I collagen (0.3 mg/mL; Nitta Gelatin, Osaka, Japan). The culture medium included Dulbecco's modified Eagle medium (DMEM)/F-12 supplemented with 10% fetal bovine serum, 5 mmol/L HEPES (Wako, Osaka, Japan), 200 μmol/L L-glutamine (Invitrogen Life Technologies), 50 μmol/L 2-mercaptoethanol (Sigma-Aldrich), 10 mmol/L nicotinamide (Sigma-Aldrich), 10^{-7} mol/L dexamethasone (Sigma-Aldrich), 1 mg/L insulin (Wako), 1× penicillin/streptomycin (Invitrogen Life Technologies), 50 ng/mL HGF (Peprotech, Rocky Hill, NJ), and 20 ng/mL EGF (Sigma-Aldrich).

Immunohistochemical analyses

Adult liver tissues were fixed with 4% paraformaldehyde at 4°C overnight and embedded in paraffin. Frozen sections were sliced and then fixed with 4% paraformaldehyde. The following primary antibodies were used: goat anti-NS (1:200; R&D Systems, Inc., Minneapolis, MN), rabbit anti-GFP (1:500; Invitrogen Life Technologies), and mouse anti-Ki-67 (1:200; BD Pharmingen). Sections were incubated with primary antibodies for 16 h at 4°C, followed by incubation with the appropriate Alexa Fluor dye conjugated to anti-goat IgG, anti-rabbit IgG, or anti-mouse IgG secondary antibodies (all 1:200; Molecular Probes, Inc., Eugene, OR). Staining was visualized using confocal microscopy (FV1000; Olympus, Tokyo, Japan). For some experiments, primary antibodies were detected using peroxidase-conjugated secondary antibodies (GE Healthcare, Amersham, Buckinghamshire, UK) in combination with a 3, 3'-diaminobenzidine (DAB) Peroxidase Substrate Kit (Vector Laboratories, Burlingame, CA). Sections were counterstained with Mayer's hematoxylin and analyzed using a microscope (Ax80; Olympus).

Immunocytochemical analyses

Hepatic colonies or cell lines were fixed with 4% paraformaldehyde for 10 min, followed by incubation with goat anti-albumin (1:100; Bethyl Laboratories, Montgomery, TX),

rabbit anti-cytokeratin 19 (1:1,000, a gift from Dr. Atsushi Miyajima), chicken anti-GFP (1:500; AVES, Tigard, OR), and/or mouse anti-Ki-67 (1:200; BD Pharmingen) at 4°C overnight and then stained with Alexa 546–conjugated and/or Alexa 488–conjugated secondary antibodies.

Western blotting analyses

Liver samples were lysed with sodium dodecyl sulfate (SDS)–polyacrylamide gel electrophoresis (PAGE) sample buffer, sonicated, boiled, and used as total liver cell lysates. Protein concentrations were measured by the bicinchoninic acid (BCA) protein assay (Pierce, Rockford, IL), and equal amounts of protein were separated by SDS-PAGE and transferred onto polyvinylidene difluoride (PVDF) membranes. Membranes were blocked with 5% skim milk in PBS containing Tween 20 for 1 h at room temperature. Membranes were then incubated with a goat anti-NS antibody (1:1,000; Neuromics, Edina, MN) for 16 h at 4°C and a mouse anti-β-actin antibody (1:1,000; Sigma-Aldrich) for 1 h at room temperature. Immune complexes were detected using peroxidase-conjugated secondary antibodies (1:1,000; GE Healthcare and DAKO, Glostrup, Denmark) for 30 min at room temperature and the ECL Prime western blotting detection system (GE Healthcare).

Reverse transcription–polymerase chain reaction

An RNeasy Mini Kit (Qiagen GmbH, Germany) was used in accordance with the manufacturer's instructions to extract total RNA from nonparenchymal cells sorted by fluorescence-activated cell sorting from adult mice treated with DDC. The primers used were as follows: GAPDH (5′-ACCA CAGTCCATGCCATCAC-3′ and 5′-TCCACCACCCTGTTG CTGTA-3′), NS (5′-TCGGAGTCCAGCAAGCATTG-3′ and 5′-GCAGCACTTTCCACATTTGGG-3′), CK19 (5′-GTCCTAC AGATTGACATTGC-3′ and 5′-CACGCTCTGGATCTGTGA CAG-3′), EpCAM (5′-AGGGGCGATCCAGAACAACG-3′ and 5′-ATGGTCGTAGGGGCTTTCTC-3′), Prominin1 (5′-GTA CCTCAGATCCAGCCAGCAA-3′ and 5′-ATTCTTCCAGCT

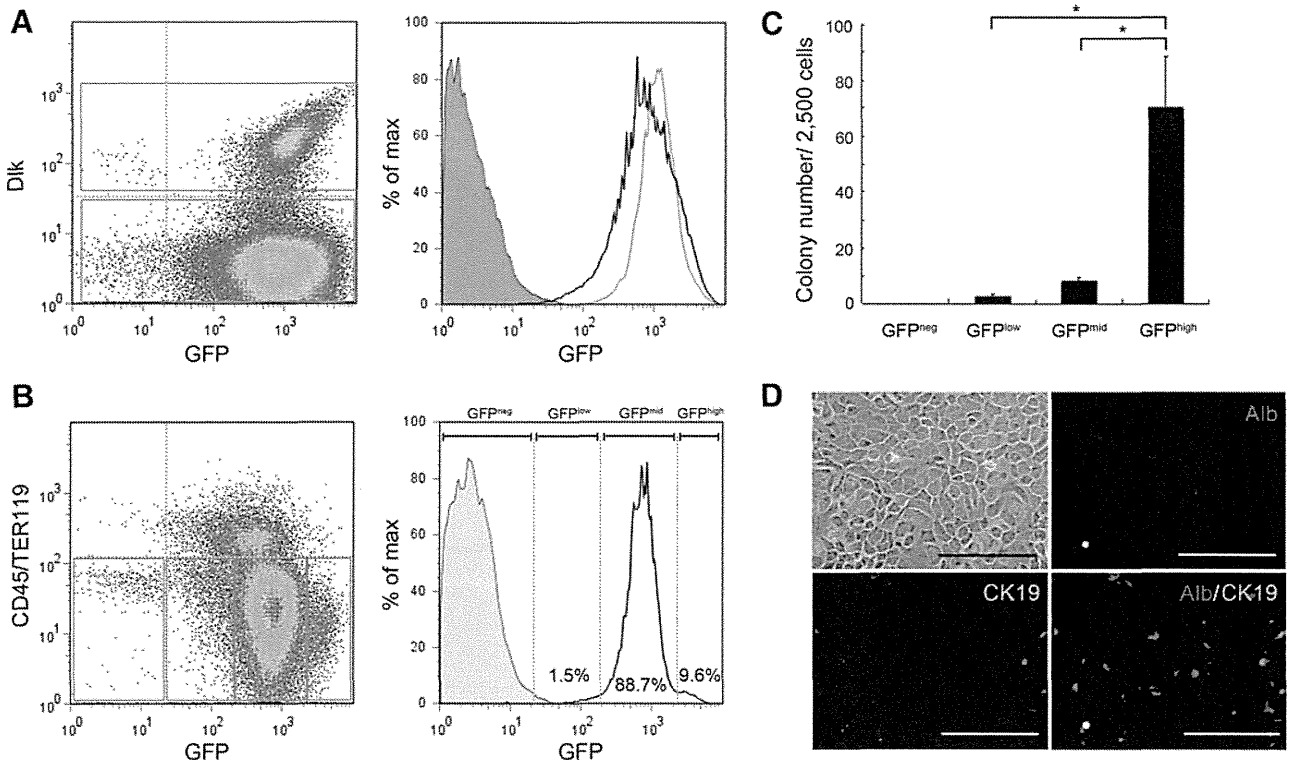

FIG. 1. Correlation of nucleostemin (NS) expression with colony-forming capacity of hepatic precursor cells in developing liver. **(A)** Flow cytometry analysis of green fluorescent protein (GFP) expression in NS-GFP Tg fetal liver. Nonhematopoietic cells from fetal liver cells at E14.5 were isolated by depletion of $CD45^+Ter119^+$ cells. *Left panel*: flow cytometry analysis of Dlk and GFP in $CD45^-Ter119^-$cells. *Right panel*: histogram of GFP expression. GFP expression in Dlk^+ cells (*gray line*) was slightly higher than that seen in Dlk^- cells (*black line*). *Gray region*: wild-type control mouse. The data shown are representative of 3 independent experiments. **(B)** Flow cytometry analysis of GFP expression in NS-GFP Tg neonatal liver. Flow cytometry analysis with CD45/Ter119 and GFP, and histogram with GFP in $CD45^-Ter119^-$ (nonhematopoietic cells) from neonatal liver (P5) are shown in the *left* and *right panels*, respectively. Nonhematopoietic cells ($CD45^-Ter119^-$) were fractionated into GFP^{neg}, GFP^{low}, GFP^{mid}, and GFP^{high} subpopulations. Values in panels are the percentage of the specified subpopulation among $CD45^-Ter119^-$ cells. The data shown are representative of 5 independent experiments. **(C)** Hepatic colony formation of subpopulations in **(B)**. Fractionated cells in **(B)** were cultured for 5 days. Data shown are the mean number ± standard deviation (SD) of colonies ($n = 3$). $^*P < 0.01$ **(D)** Characterization of hepatic colonies. Colonies (brightfield, *upper left panel*) were fixed and stained with anti-albumin (*red*) and anti-CK19 (*green*) antibodies. Most colonies in the culture express albumin or CK19. Representative data are shown. Scale bars, 100 μm.

TGGGCAGC-3'), and CD44 (5'-GGCTTTCAACAGTACC TTAC-3' and 5'-TGAAGCAATATGTGTCATAG-3').

Lentiviral transduction of short hairpin RNA

To downregulate NS in hepatic precursor cells or mouse hepatic cell lines (Hepa1-6, a mouse hepatocellular carcinoma cell line and BNL C1. 2, a mouse embryonic liver cell line), lentiviruses carrying short hairpin RNA (shRNA) against NS was prepared as previously described [14]. Oligonucleotides encoding shRNA directed against mouse NS mRNA were synthesized as follows: NS #1: sense, AGTAGA AATTTGATGGGCA; antisense, AGCAGAAACTTGATAG GCA; NS #2: sense, GAGGAAAGTTGTTTCGTTA; antisense, GAAGAAAGTTGTTCCATTA. Hepatic colonies derived from Dlk^+ fetal liver cells or cell lines were infected with lentivirus for 12 h, followed by washes with PBS, and incubation with culture medium. Cell lines were cultured with 10% FCS/DMEM (Invitrogen Life Technologies).

NS knockdown by hydrodynamic shRNA injection

In vivo transfection of shRNA plasmids into hepatocytes was performed by hydrodynamic injection using 6-week-old mice 3 days prior to partial hepatectomy, in accordance with a previous report [20]. A 27-gauge needle was used to inject 40 μg of plasmid in 2 mL PBS through the tail vein within 10 s. Three days later, the animals were sacrificed and the livers were fixed with 4% paraformaldehyde in PBS and embedded in paraffin for sectioning.

Statistical analyses

Statistical differences were determined using the unpaired Student's *t*-test for *P* values.

Results

NS expression correlates with the colony-forming capacity of hepatic precursor cells in developing liver

To investigate NS expression in developing liver, we evaluated GFP intensity in liver cells of NS-GFP Tg fetuses (E14.5) and neonates (P5). Flow cytometry analysis of fetal liver cells showed that most $CD45^-Ter119^-$ (non-hematopoietic) cells expressed high GFP levels (Fig. 1A). Although GFP levels were very high in Dlk^+ cells, in which hepatic stem/precursor cells are enriched [21], those levels were only slightly higher than those in Dlk^- cells (Fig. 1A). Thus, GFP expression was not indicative of a particular subpopulation in fetal liver. Interestingly, however, NS-GFP neonatal liver cells fell into distinct populations based on GFP

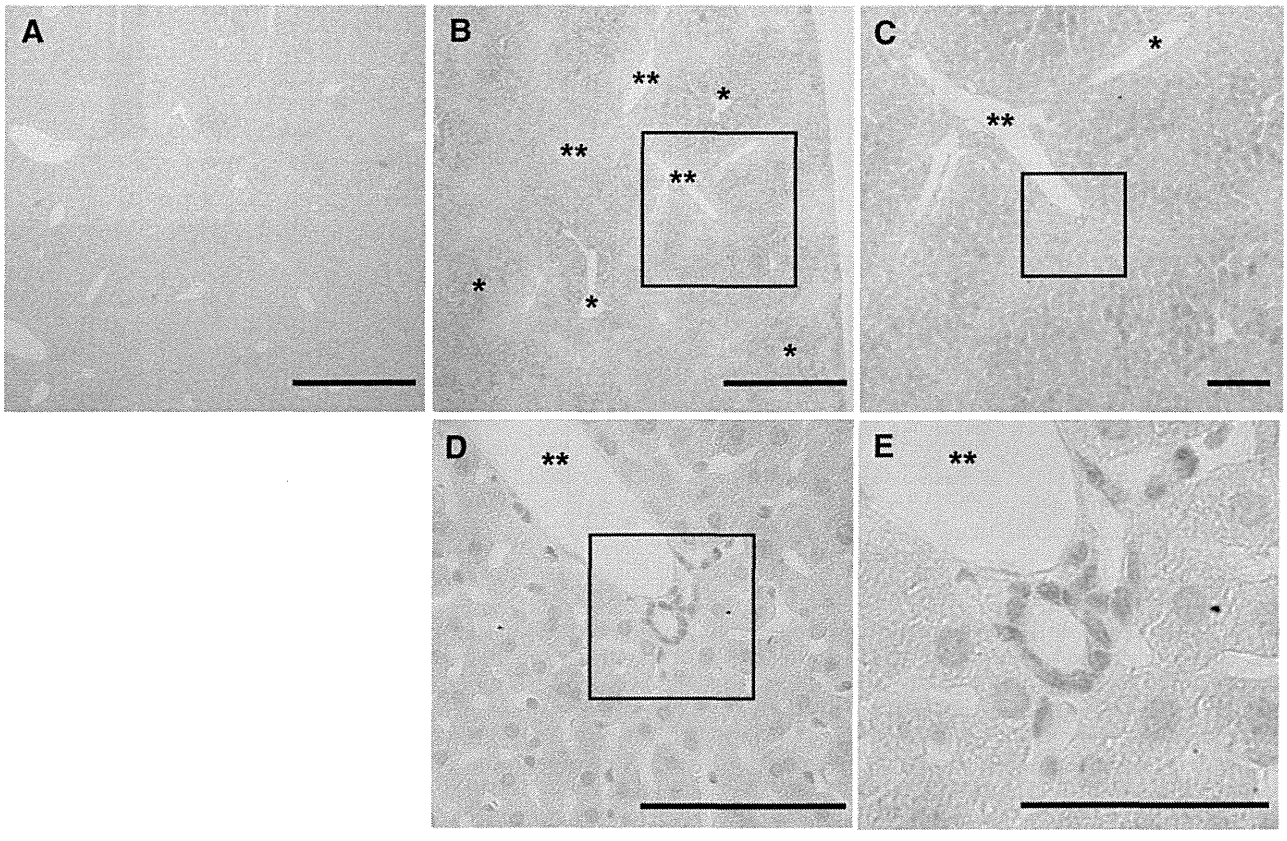

FIG. 2. Expression of NS-GFP in hepatocytes and bile duct epithelial cells of adult liver. **(A–E)** Immunohistochemical analyses of GFP in livers of adult mice (8 weeks old). Sections were stained with an anti-GFP antibody (*brown*), followed by a 3, 3'-diaminobenzidine (DAB) peroxidase reaction. **(A)** Wild-type control (C57BL/6) mice. **(B–E)** NS-GFP Tg mice. **(B)**, **(C)**, and **(D)** are lower-power views of areas shown at higher power in **(C)**, **(D)**, and **(E)**, respectively. Scale bars, 500 μm **(A, B)**, 100 μm **(C, D)**, 50 μm **(E)**, *central vein, **portal vein.

fluorescence intensity (Fig. 1B). While most non-hematopoietic cells were GFP^{mid}, we found a distinct GFP^{high} population. The proportions of GFP^{low} and GFP^{neg} cells were very small. To determine the potential functional significance of these subpopulations, we evaluated hepatic colony forming ability. GFP^{high} cells generated colonies at higher frequency than did any other cell population (Fig. 1C). Most colonies derived from GFP^{high} cells were $CK19^{+}$ or $albumin^{+}$ hepatocytes (Fig. 1D), suggesting that NS is an indicator of hepatic precursor cells in neonatal liver.

Partial hepatectomy upregulates NS expression in hepatocytes

We next examined NS-GFP expression in adult liver. We found that NS-GFP is highly expressed in hepatocytes. In

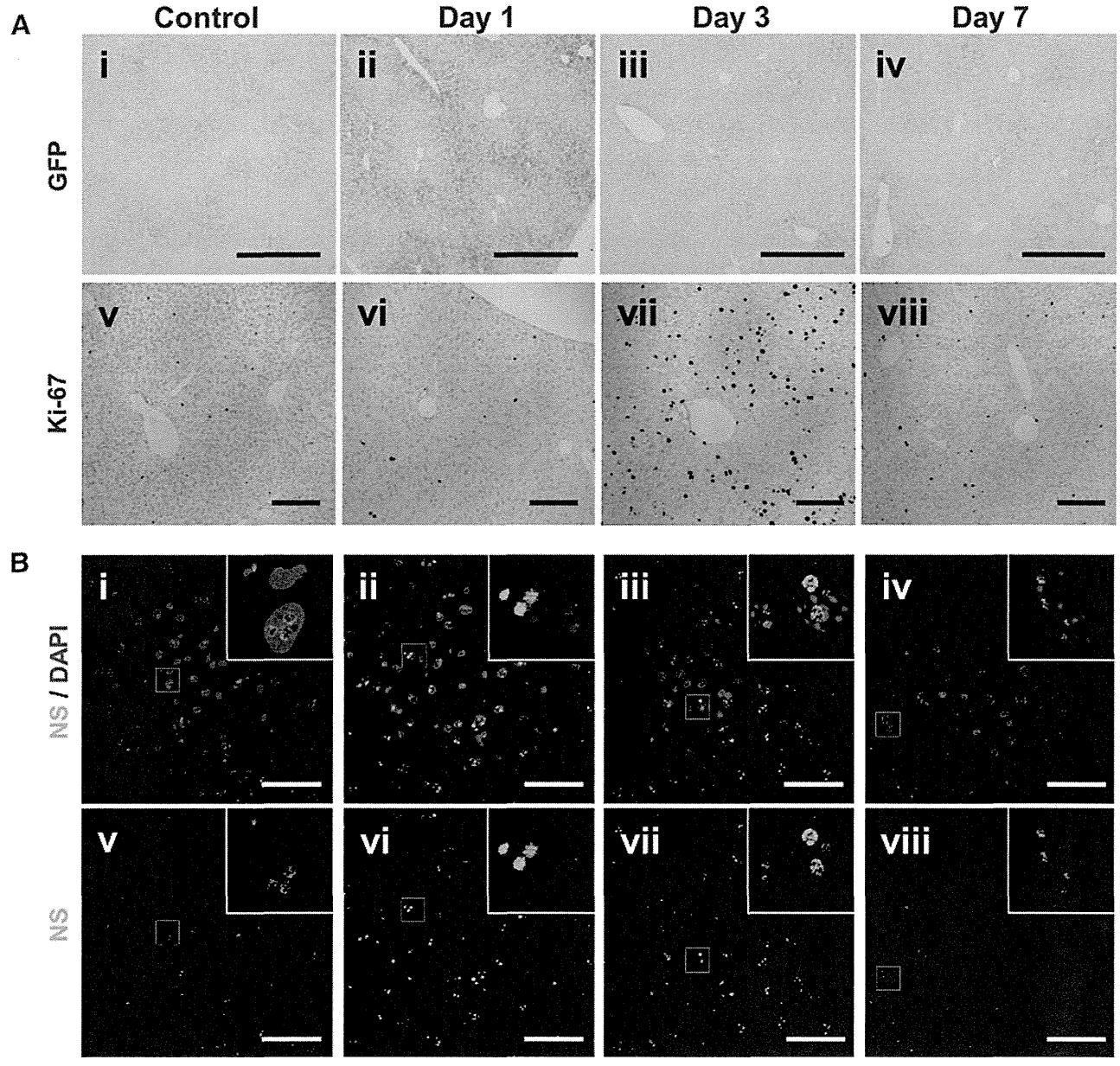

FIG. 3. Upregulation of NS-GFP in adult hepatocytes in response to partial hepatectomy. **(A)** Immunohistochemical analyses of GFP in liver of adult NS-GFP Tg mice after partial hepatectomy. Sections were stained with anti-GFP **(i–iv,** *brown***)** or anti-Ki-67 antibodies **(v–viii,** *brown***)**, followed by DAB peroxidase reactions. **(i, v)** control, **(ii, vi)** day 1, **(iii, vii)** day 3, **(iv, viii)** day 7. Scale bars, 500 μm **(i–iv)**, 100 μm **(v–viii)**. **(B)** Immunohistochemical analyses of endogenous NS in liver of adult NS-GFP Tg mice after partial hepatectomy. Liver sections were stained with an anti-NS antibody, followed by a secondary antibody conjugated to Alexa 488 **(***green***, i–viii)** plus DAPI **(**nuclear staining, *blue*, **i–iv)**. **(i, v)** control, **(ii, vi)** day 1, **(iii, vii)** day 3, **(iv, viii)** day 7. Scale bars, 50 μm. *Insets* are magnified views of the indicated areas. **(C)** Western blotting analyses of endogenous NS in liver of adult wild-type mice after partial hepatectomy. Lysates were prepared from liver (3 independent samples for each group) and immunoblotted to detect NS and β-actin as a loading control. Short and long exposures are shown for NS in the *upper* and *middle panels*, respectively.

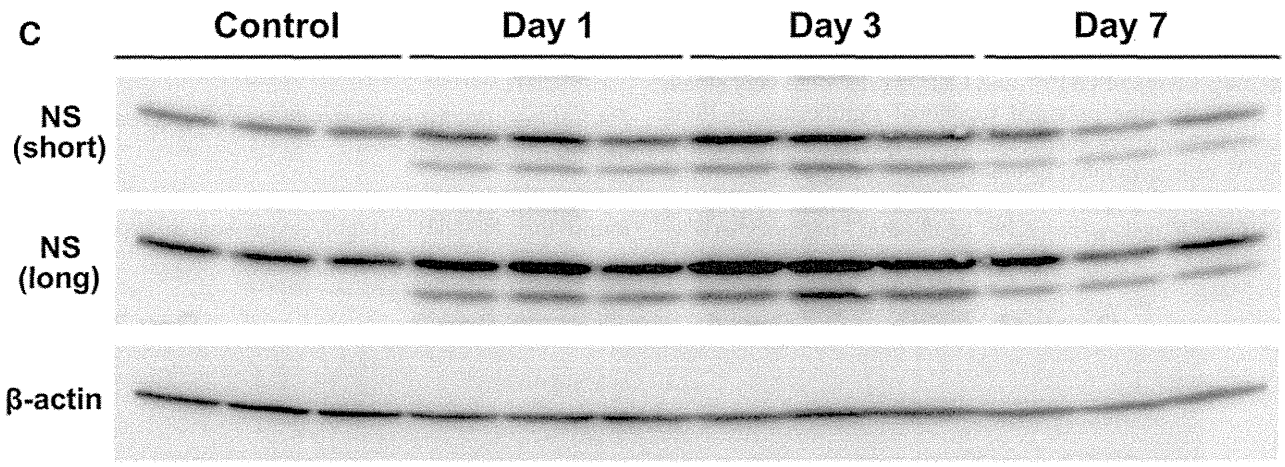

FIG. 3. (Continued).

particular, hepatocytes near central veins showed higher levels of NS-GFP expression than did those in the portal area (Fig. 2A–C). In addition, we found that NS-GFP is also highly expressed in bile duct epithelial cells (Fig. 2D, E). Next, we asked whether expression levels of NS-GFP are altered by liver injury. After partial hepatectomy, NS-GFP was upregulated within 24 h (Fig. 3A i–iv). Immunohistochemical analyses showed that NS protein expression was remarkably increased in nucleoli 24 h after hepatectomy. Although there were variations among samples, NS protein levels appeared to remain elevated at day 3 (Fig. 3B) and reverted to baseline levels at day 7, whereas NS-GFP expression was already downregulated at day 3. Western blotting analysis using an anti-NS antibody consistently showed an increase in endogenous NS protein on day 1 and day 3 after partial hepatectomy (Fig. 3C). The discrepancy between NS-GFP and endogenous NS is possibly due to differences in protein stability stemming from different post-translational modification of these molecules. Interestingly, partial hepatectomy induced a variant form of NS that is reported to be expressed in particular tissues [22,23]. Hepatocytes that had begun to proliferate showed a small increase in the expression of Ki-67, a marker of cell proliferation, at day 1, and further increases in Ki-67 expression were observed at day 3 (Fig. 3A v–viii). These data indicate that NS gene expression is rapidly upregulated before the start of cell division in response to partial hepatectomy.

A DDC diet induces emergence of ductal epithelial cells expressing NS-GFP

DDC treatment inhibits the capacity for hepatocytes to regenerate, while inducing ductal proliferation in mice in what is known as the oval cell response [6]. We found that DDC treatment reduced expression of NS-GFP in hepatocytes (Fig. 4A i, ii) compared to the expression in untreated hepatocytes. We also found that bile duct-like NS-GFP-positive cells emerged in the portal zone following DDC treatment (Fig. 4A iii, iv). Interstitial cells surrounding ductal cells did not express NS-GFP. We confirmed by immunofluorescence that NS-GFP was expressed in $CK19^+$ ductal epithelial cells (Fig. 4B). To investigate the regenerative capacity of NS-GFP-expressing cells in DDC-treated liver, we evaluated NS-GFP intensity in nonparenchymal cells, since oval cells reportedly reside in that population [6]. Flow cytometry analysis showed that most $CD45^-Ter119^-$ nonparenchymal cells were GFP-positive (Fig. 5A), although the intensity of NS-GFP expression in non-parenchymal cells in adult mice appeared lower than that seen in developing liver cells. These NS-GFP-positive cells fell into GFP^{high} and GFP^{low} populations. GFP^{high} cells were relatively rare, but only GFP^{high} cells showed hepatic colony forming ability (Fig. 5C). In contrast, no colonies were generated from GFP^{low} or GFP^{neg} cells. Severe liver injury promoted by a DDC diet increased the proportion of GFP^{high} cells relative to the proportion in untreated mice (Fig. 5B). Because we found that ductal cells express NS-GFP (Figs. 2 and 4), we assumed that the DDC diet increased the number of ductal cells, resulting in an increase in the proportion of GFP^{high} cells. Hepatic colonies were generated only from GFP^{high} cells (Fig. 5D). GFP^{high} cells expressed higher levels of NS mRNA, indicating that GFP expression corresponded with that of endogenous NS, and also expressed several genes reportedly expressed in oval cells [19] (Fig. 5E). These data indicate that hepatic precursor cells induced by severe liver injury express NS.

NS downregulation inhibits proliferation of hepatic precursor cells

Next, to address whether NS is required for regeneration of hepatic precursor cells, we downregulated NS expression in hepatic cell line and primary fetal liver cells in vitro. Previously, we successfully suppressed NS in a germ cell line by infection with a lentivirus carrying NS shRNA [14]. In this system, infected cells were identified by GFP expression driven by the lentivirus vector (GFP^+ cells). For the current study, we infected the mouse hepatocellular carcinoma cell line Hepa1-6 and the mouse embryonic liver cell line BNL C1.2 with lentiviruses carrying NS shRNA (#1 or #2) or a scrambled control shRNA and then stained the cells with an anti-NS antibody. Both shRNAs, but not the scrambled control, efficiently reduced expression of NS protein in the hepatic cell lines (Fig. 6A, data not shown). NS knockdown (GFP^+) cells in the cell lines had dramatically reduced colony-forming capacity (Fig. 6B, data not shown). We also found that NS downregulation significantly decreased the